A new kentriodontid (Cetacea: Odontoceti) from the early to middle Miocene of the western North Pacific and a revision of kentriodontid phylogeny (#52427)

First revision

Guidance from your Editor

Please submit by 27 Dec 2020 for the benefit of the authors .



Structure and Criteria

Please read the 'Structure and Criteria' page for general guidance.



Custom checks

Make sure you include the custom checks shown below, in your review.



Raw data check

Review the raw data.



Image check

Check that figures and images have not been inappropriately manipulated.

Privacy reminder: If uploading an annotated PDF, remove identifiable information to remain anonymous.

Files

Download and review all files from the <u>materials page</u>.

- 1 Tracked changes manuscript(s)
- 1 Rebuttal letter(s)
- 14 Figure file(s)
- 1 Table file(s)
- 5 Other file(s)

Custom checks

New species checks

- Have you checked our new species policies?
- Do you agree that it is a new species?
- Is it correctly described e.g. meets ICZN standard?

Structure and Criteria



Structure your review

The review form is divided into 5 sections. Please consider these when composing your review:

- 1. BASIC REPORTING
- 2. EXPERIMENTAL DESIGN
- 3. VALIDITY OF THE FINDINGS
- 4. General comments
- 5. Confidential notes to the editor
- Prou can also annotate this PDF and upload it as part of your review

When ready <u>submit online</u>.

Editorial Criteria

Use these criteria points to structure your review. The full detailed editorial criteria is on your guidance page.

BASIC REPORTING

- Clear, unambiguous, professional English language used throughout.
- Intro & background to show context.
 Literature well referenced & relevant.
- Structure conforms to <u>PeerJ standards</u>, discipline norm, or improved for clarity.
- Figures are relevant, high quality, well labelled & described.
- Raw data supplied (see <u>PeerJ policy</u>).

EXPERIMENTAL DESIGN

- Original primary research within Scope of the journal.
- Research question well defined, relevant & meaningful. It is stated how the research fills an identified knowledge gap.
- Rigorous investigation performed to a high technical & ethical standard.
- Methods described with sufficient detail & information to replicate.

VALIDITY OF THE FINDINGS

- Impact and novelty not assessed.
 Negative/inconclusive results accepted.
 Meaningful replication encouraged where rationale & benefit to literature is clearly stated.
- All underlying data have been provided; they are robust, statistically sound, & controlled.
- Speculation is welcome, but should be identified as such.
- Conclusions are well stated, linked to original research question & limited to supporting results.

Standout reviewing tips



The best reviewers use these techniques

Τ	p

Support criticisms with evidence from the text or from other sources

Give specific suggestions on how to improve the manuscript

Comment on language and grammar issues

Organize by importance of the issues, and number your points

Please provide constructive criticism, and avoid personal opinions

Comment on strengths (as well as weaknesses) of the manuscript

Example

Smith et al (J of Methodology, 2005, V3, pp 123) have shown that the analysis you use in Lines 241-250 is not the most appropriate for this situation. Please explain why you used this method.

Your introduction needs more detail. I suggest that you improve the description at lines 57-86 to provide more justification for your study (specifically, you should expand upon the knowledge gap being filled).

The English language should be improved to ensure that an international audience can clearly understand your text. Some examples where the language could be improved include lines 23, 77, 121, 128 - the current phrasing makes comprehension difficult.

- 1. Your most important issue
- 2. The next most important item
- 3. ...
- 4. The least important points

I thank you for providing the raw data, however your supplemental files need more descriptive metadata identifiers to be useful to future readers. Although your results are compelling, the data analysis should be improved in the following ways: AA, BB, CC

I commend the authors for their extensive data set, compiled over many years of detailed fieldwork. In addition, the manuscript is clearly written in professional, unambiguous language. If there is a weakness, it is in the statistical analysis (as I have noted above) which should be improved upon before Acceptance.



A new kentriodontid (Cetacea: Odontoceti) from the early to middle Miocene of the western North Pacific and a revision of kentriodontid phylogeny

Zixuan Guo Corresp., 1, Naoki Kohno 1, 2

Corresponding Author: Zixuan Guo Email address: guo_z@geol.tsukuba.ac.jp

A new species of an extinct dolphin belonging to the kentriodontids, i.e., Kentriodon sugawarai sp. nov., is described from the late early to earliest middle Miocene Kadonosawa Formation in Ninohe City, Iwate Prefecture, northern Japan. The holotype of *Kentriodon* sugawarai sp. nov., consists of a partial skull with ear bones, mandibular fragments, and some postcranial bones. This new species shares five unique characters with other species of Kentriodon. In addition, the new species differs from other species of the genus in displaying a narrow width of the squamosal lateral to the exoccipital in posterior view, the dorsolateral edge of the opening of the ventral infraorbital foramen that is formed by the maxilla and the lacrimal or the jugal, and at least three anterior dorsal infraorbital foramina. Our phylogenetic analysis based on 393 characters for 103 Odontoceti taxa, yielded a consensus showing all previously identified kentriodontids as a monophyletic group that comprises the sister group of the crown Dephinoidea, which in turn include Delphinidae, Phocoenidae and Monodontidae. Our analysis also indicates that the distinct renewal of the acoustic apparatus (i.e., 13 out of 29 derived characters are from tympanoperiotic) would have occurred in the Delphinoidea with the monophyletic Kentriodontidae during their evolution and diversification.

¹ Faculty of Life and Environmental Sciences, University of Tsukuba, Tsukuba, Japan

² Department of Geology and Paleontology, National Museum of Nature and Science, Tsukuba, Japan



1 A new kentriodontid (Cetacea: Odontoceti) from the 2 early to middle Miocene of the western North Pacific and a revision of kentriodontid phylogeny 5 6 Zixuan Guo¹, Naoki Kohno^{1,2} 7 8 ¹ Faculty of Life and Environmental Sciences, University of Tsukuba, Tsukuba, Japan 9 ² Department of Geology and Paleontology, National Museum of Nature and Science, Tsukuba, 10 11 Japan 12 13 Corresponding Author: Zixuan Guo¹ 14 University of Tsukuba, 1-1-1 Tennodai, Tsukuba, 305-8577, Japan 15 Email address: guo z@geol.tsukuba.ac.jp 16 17



Abstract

- 19 A new species of an extinct dolphin belonging to the kentriodontids, i.e., Kentriodon sugawarai
- sp. nov., is described from the late early to earliest middle Miocene Kadonosawa Formation in 20
- Ninohe City, Iwate Prefecture, northern Japan. The holotype of *Kentriodon sugawarai* sp. nov., 21
- 22 consists of a partial skull with ear bones, mandibular fragments, and some postcranial bones.
- This new species shares five unique characters with other species of *Kentriodon*. In addition, the 23
- 24 new species differs from other species of the genus in displaying a narrow width of the
- squamosal lateral to the exoccipital in posterior view, the dorsolateral edge of the opening of the 25
- 26 ventral infraorbital foramen that is formed by the maxilla and the lacrimal or the jugal, and at
- least three anterior dorsal infraorbital foramina. Our phylogenetic analysis based on 393 27
- characters for 103 Odontoceti taxa, yielded a consensus showing all previously identified 28
- kentriodontids as a monophyletic group that comprises the sister group of the crown 29
- 30 Dephinoidea, which in turn include Delphinidae, Phocoenidae and Monodontidae. Our analysis
- also indicates that the distinct renewal of the acoustic apparatus (i.e., 13 out of 29 derived 31
- 32 characters are from tympanoperiotic) would have occurred in the Delphinoidea with the
- monophyletic Kentriodontidae during their evolution and diversification. 33

34 35

52

Introduction

- Dephinoidea (i.e., Delphinidae, Monodontidae and Phocoenidae) has been thought to emerge in 36
- the early Miocene (Gatesy et al., 2013) and they are the most species-rich group of living marine 37
- mammal clade in the world. However, their evolutionary origins are still puzzling. Proceeding in 38
- 39 the dawn of Dephinoidea, small coastal odontocetes known as kentriodontids (Barnes &
- Mitchell, 1984; Barnes, 1985; Muizon, 1988a) attained a high diversity during the period 40
- between the early and the late Miocene (Ichishima et al., 1995; Kazár & Hampe, 2014; Peredo, 41
- Uhen, & Nelson, 2018). This group had been considered to be placed in the stem delphinoids 42
- 43 based on their primitive cranial morphologies and retention of several ancestral character states
- 44 of odontocetes (Barnes, 1978). For instance, asymmetric nasals and premaxillae have commonly
- been observed in modern odontocetes. However, in part of the taxa referred to as members of 45
- 46 kentriodontids, these bones are seemingly symmetrical. The interpretation of the evolutionary
- patterns of the Delphinoidea greatly relies upon the processes of morphological transformation in 47
- 48 their stem group, while the phylogenetic relationships of such a stem group, presumably the
- kentriodontids, have remained debated. 49

50 51

In the initial stage of the studies on kentriodontids, they were considered as comprising a monophyletic family, i.e., Kentriodontidae (e.g., Barnes, 1978; Barnes, 1985; Muizon, 1988a,

1988b; Ichishima et al., 1995). However, recent studies have advocated that 'kentriodontids' are

- 53 paraphyletic and should be subdivided into several clades by a different combination of taxa
- 54 within Delphinida (including Lipotidae, Inioidea, and Delphinoidea) as in a broad sense (e.g.,
- Lambert et al., 2017; Peredo, Uhen & Nelson, 2018; Kimura & Hasegawa, 2019). Because 55
- 56 several additional specimens of 'kentriodontids' have recently reported, and molecular
- phylogenies of the cetaceans have been established in the last decade (e.g., McGowen, Spaulding 57



- 58 & Gatesy, 2009; McGowen et al., 2011; McGowen et al., 2020; Geisler et al., 2011), a more
- 59 comprehensive reappraisal of the phylogeny of this group is necessary. In particular, Peredo,
- 60 Uhen & Nelson (2018) redefined the family Kentriodondae, only including Wimahl,
- 61 Kampholophos and Kentriodon. However, some other phylogenetic studies (e.g., Murakami et
- 62 al., 2014; Tanaka & Fordyce, 2014, 2016; Tanaka et al., 2017; Lambert et al., 2018), using
- 63 different character sets and data matrices displayed some kentriodontid taxa in a different
- 64 phylogenetic topology. In other words, the relationships of taxa originally referred to the family

65 'Kentriodontidae' are still debated (Fig. 1).

Here, we describe a new species of kentriodontid from the early to middle Miocene of Japan (Fig. 2). The holotype specimen includes a partial skull with well-preserved tympanoperiotics. We also reassess the phylogenetic relationships of kentriodontids and debate on the evolution of Delphinoidea, including kentriodontids.

70 71

72

66

67

68

69

Materials & Methods

Nomenclatural acts

- 73 The electronic version of this article in Portable Document Format (PDF) will represent a
- 74 published work according to the International Commission on Zoological Nomenclature (ICZN),
- and hence the new names contained in the electronic version are effectively published under that
- 76 Code from the electronic edition alone. This published work and the nomenclatural acts it
- 77 contains have been registered in ZooBank, the online registration system for the ICZN. The
- 78 ZooBank LSIDs (Life Science Identifiers) can be resolved and the associated information viewed
- 79 through any standard web browser by appending the LSID to the prefix http://zoobank.org/. The
- 80 LSID for this publication is: urn:lsid:zoobank.org:pub:B0E9467F-CDD3-4AF4-83FE-
- 81 40CE09D15700. The online version of this work is archived and available from the following
- 82 digital repositories: PeerJ, PubMed Central and CLOCKSS

83 84

Anatomical terminology

We follow Mead & Fordyce (2009) and Ichishima (2016) for the terminology of skull.

85 86 87

Phylogenetic Methods

- 88 The phylogenetic position of the new specimen described here was analyzed based on a character
- 89 list and the character matrix that stems from the works by Tanaka et al. (2017) and Lambert et al.
- 90 (2017). The character list and data matrix by Tanaka et al. (2017) derive from those by Geisler et
- al. (2011) via the addition of characters by Murakami et al. (2012) to understand interspecific
- 92 relationships of the Phocoenidae within the crown Delphinoidea, and the subsequent
- 93 modifications by Tanaka & Fordyce (2014). The data matrix by Tanaka et al. (2017) included 87
- 94 taxa and 284 characters, but this matrix only included 3 kentriodontid taxa: i.e., Atocetus iquensis
- 95 Muizon 1988b, *Hadrodelphis calvertense* Dawson 1996a, and *Kentriodon pernix* Kellogg 1927.
- 96 By contrast, the data matrix by Lambert et al. (2017) was also based on Geisler et al. (2011) and
- 97 Geisler, Godfrey & Lambert (2012), but it included 112 taxa and 324 characters, with 12



- 98 kentriodontid taxa: i.e., Atocetus iauensis, Atocetus nasalis Muizon 1988b, Delphinodon dividum True 1912, Hadrodelphis calvertense, Kampholophus serrulus Rensberger 1969, Kentriodon 99 pernix, Lophocetus calvertensis Cope 1867, Lophocetus repenningi Barnes 1978, 100 Macrokentriodon morani Dawson 1996b, Pithanodelphis cornutus Abel 1905, Rudicetus 101 102 squalodontoides Bianucci 2001, and Tagicetus joneti Lambert, Estevens & Smith 2005. However, the character set used by Lambert et al. (2017) for their phylogenetic analysis was 103 originally elaborated for the taxa within much basal branching clades of the Odontoceti (e.g., 104 Geisler et al., 2011; Lambert et al., 2017; Peredo, Uhen & Nelson, 2018; Kimura & Hasegawa, 105 2019). Consequently, the focus of these two streams of studies on the odontocete phylogeny 106 (e.g., Tanaka et al., 2017 and e.g., Lambert et al., 2017) have not overlapped with each other, in 107 other words, the included taxa of kentriodontids and character combination to analyze their 108 phylogenetic relationships were far too different to each other. To solve these issues, we 109 elaborated a phylogenetic dataset based on the combined characters and kentriodontid taxa from 110 111 previous studies such as Geisler, Godfrey & Lambert (2012), Murakami et al. (2012), Tanaka & Fordyce (2014), Tanaka et al. (2017), Lambert et al. (2017), Peredo, Uhen & Nelson (2018), and 112 Kimura & Hasegawa (2019). The resulting data matrix of that is used herein is based on 103 113 taxa, including almost all kentriodontids, and 393 morphological characters (see Supplemental 114 115 Information), with a tree constraint based on the molecular phylogenetic studies of the extant cetaceans by McGowen, Spaulding & Gatesy (2009), McGowen et al. (2011) and McGowen et 116 al. (2020). As regarding to the kentriodontids, we included the following 15 taxa into our data 117 matrix (see also Supplemental Information): Atocetus nasalis from the late Miocene of 118 California, USA (Muizon, 1988b), Delphinodon dividum from the early Miocene of Meryland, 119 120 USA (True, 1912), Kampholophos serrulus from the early Miocene of California, USA (Rensberger, 1969), Kentriodon diusinus Salinas-Márquez et al. 2014 from the middle Miocene 121 of Baja California, Mexico (Salinas-Márquez et al., 2014), Kentriodon nakajimai Kimura & 122 Hasegawa 2019 from the middle to late Miocene of Japan (Kimura & Hasegawa, 2019), 123 124 Kentriodon obscurus Kellogg 1931 from the middle Miocene of California, USA (Kellogg, 1931; Barnes & Mitchell, 1984), Kentriodon schneideri Whitmore & Kaltenbach 2008 from the 125 middle Miocene of North Carolina, USA (Whitmore & Kaltenbach, 2008), Liolithax pappus 126 from the middle Miocene of Maryland, USA (Barnes, 1978), Lophocetus calvertensis from the 127 128 late Miocene of Maryland, USA (Cope, 1867), Lophocetus repenningi from the middle Miocene of California, USA (Barnes, 1978), Macrokentriodon morani from the middle Miocene of 129 Maryland, USA (Dawson, 1996b), Pithanodelphis cornutus from the late Miocene of Belgiun 130 (Flower, 1872), Rudicetus squalodontoides from the early to late Miocene of Italy (Bianucci, 131 2001), Tagicetus joneti from the middle Miocene of Portugal (Lambert, Estevens & Smith, 132 2005), and Wimahl chinookensis Peredo, Uhen & Nelson 2018 from the early Miocene of 133
- The phylogenetic analysis was performed with TNT 1.5 (Goloboff, Farris & Nixon, 2008; Goloboff & Catalano, 2016). All characters were treated as unweighted and unordered,
- using the "New Technology Search" task to find minimum length trees 1,000 times, under a tree

Washington, USA (Peredo, Uhen & Nelson, 2018).



constraint based on molecular evidence from the extant taxa (McGowen, Spaulding & Gatesy, 2009; McGowen et al., 2011; McGowen et al., 2020).

140141

SYSTEMATIC PALEONTOLOGY

142

- 143 CETACEA Brisson, 1762
- 144 ODONTOCETI Flower, 1867
- 145 DELPHINIDA Muizon, 1988a
- 146 KENTRIODONTIDAE Slijper, 1936

147

- 148 Emended Diagnosis of Kentriodontidae: Differing from other delphinidan families (i.e.,
- 149 Delphinidae, Phocoenidae, Monodontidae, Lipotidae, and Inioidea) in displaying the following
- suite of derived character states: premaxillae are compressed mediolaterally at anterior part of
- 151 the rostrum (Chr. 3), the mesorostral groove constricted posteriorly, anterior to the nares and
- behind the level of the antorbital notch, then rapidly diverging anteriorly (Chr. 7), anterior edge
- of the supraorbital process is oriented anterolaterally, forming an angle between 35° and 60°
- 154 (Chr. 50), the dorsolateral edge of internal opening of the infraorbital foramen is formed by the
- lacrimal or the jugal (Chr. 58), the infratemporal crest forming a well-defined curved ridge on
- 156 the posterior edge of the sulcus for the optic nerve (Chr. 64), the premaxillary foramen is located
- medially (Chr. 72), the alisphenoid is broadly exposed laterally in the temporal fossa (Chr. 160),
- suture between both the palatines and both the maxillae is straight transversely or bowed
- anteriorly (Chr. 179), the external auditory meatus is wide (Chr. 225), the basioccipital crests
- 160 forming an angle of approximately 15–40° in ventral view (Chr. 229), the hypoglossal foramen
- is separated from the jugular foramen or the jugular notch by thick bone (Chr. 231), most convex
- part of the pars cochlearis is on the ventrolateral surface (Chr. 283).

163 164

Kentriodon Kellogg, 1927

165

- 166 **Emended Diagnosis of Genus**: *Kentriodon* differs from other genera of kentriodontids by the
- 167 following unique characters: the cheek tooth entocingulum is present (Chr. 28); the dorsal edge
- of the orbit is low, either in line with the edge of the rostrum or slightly above it (Chr. 47); the
- position of the inflection of premaxilla is located in line with the posterior half of the supraorbital
- 170 process or in line with the postorbital process of frontal (Chr. 109); in lateral view, the dorsal
- 171 edge of the zygomatic process preserves a distinct dorsal flange or process near the anterior end,
- articulates with the frontal (Chr. 164); and the postzygapophysis is appearing as a crest,
- elongated dorsolaterally from anterior view (Chr. 328). In this regard, *Rudicetus squalodontoides*
- 174 could also be included in this genus.

175

- 176 Kentriodon sugawarai sp. nov.
- 177 (Figs. 3–12, Table 1)



- 179 **LSID**: urn:lsid:zoobank.org:act:0D209916-B472-44A7-B7AB-29682FA945C4
- 180 Holotype: NMHF 999, incomplete skull including the most of the neurocranium and a proximal
- portion of the rostrum, one tooth, the right tympanoperiotics and the malleus, fragments of the
- 182 left and right mandibles, and the partial atlas.
- 183 **Diagnosis of Species**: *Kentriodon sugawarai* sp. nov. differs from *K. schneideri* by the convex
- occipital (Chr. 176). It differs from K. pernix, K. nakajimai and K. obscurus by the following
- characters: the dorsolateral edge of the opening of the ventral infraorbital foramen is formed by
- the maxilla and the lacrimal or the jugal (Chr. 58), at least three anterior dorsal infraorbital
- 187 foramina (Chr. 65), anterolateral corner of the nasal lacking a distinct inflated process (Chr. 136),
- narrow width of the squamosal lateral to the exoccipital (Chr. 170), anterior level of the
- pterygoid sinus fossa is interrupted posterior to (or at the level of) the antorbital notch (Chr. 193),
- and the ventral edge of the anterior process of the periotic is clearly concave in lateral view (Chr.
- 191 245). Further differs from *Kentriodon hoepfneri* and *K. nakajimai* by the apex of the postorbital
- process of the frontal that is directed ventrally rather than posterolaterally, by the angle between
- anterior process of periotic and anterior edge of pars cochlearis that is nearly 90 degrees. It
- differs from K. nakajimai, K. diusinus and K. schneideri by displaying a deep emargination of
- the posterior edge of the zygomatic process by the neck muscle fossa. It differs from *Kentriodon*
- 196 hobetsu, K. schneideri and K. pernix by the transversely narrower exoccipital, also by the maxilla
- that makes a pair of deep fossae at the vertex. It differs from *K. obscurus* and *K. pernix* by the
- aperture for cochlear aqueduct that is transversely smaller than the aperture for the vestibular
- aqueduct. It further differs from *K. pernix* by having a shallower lateral furrow of the tympanic
- 200 bulla.
- 201 **Etymology**: The species is named in honor of Mr. Kohei Sugawara, the former director of the
- 202 Ninohe Museum of History and Folklore, for his longstanding contributions to geology and
- 203 paleontology as well as local history of the Ninohe district, and as a sign of gratitude for his
- 204 encouragement and assistance to both of us throughout this study.
- 205 **Type Locality**: The holotype was collected in the 1940s from a locality close to the Mabechi
- 206 River, Ninohe City, Iwate Prefecture, Japan. Approximate geographical coordinates: 40°31'N.
- 207 141°31′E; (Fig. 2).
- Formation and Age: Although the precise locality of NMHF 999 is at present uncertain, and the
- 209 exact horizon from which NMHF 999 was collected is also unclear, the siltstone matrix adhering
- 210 to NMHF 999 has produced a diatom flora that includes *Denticulopsis praelauta* (Oishi et al.,
- 211 1999). Consequently, NMHF 999 should come from the middle or upper portions of the
- 212 Kadonosawa Formation, because the Shikonai Siltstone Member of this formation is dominated
- 213 by silts and very fine sandstones. The Shikonai Siltstone Member of the Kadonosawa Formation
- 214 is widely distributed in Ninohe City, including the provenance area of NMHF 999. The siltstone
- 215 layers of the Shirikonai Siltstone Member of the Kadonozawa Formation have produced richness
- of diatoms, that has been referred to the *Denticulopsis praelauta* Zone (NPD 3B) (TuZino &
- 217 Yanagisawa, 2017; Tuzino et al., 2018). The range in age of this zone spans



- 218 chronostratigraphically between 16.3 and 15.9 Ma (Yanagisawa & Akiba, 1998), latest
- 219 Burdigalian to earliest Langhian, latest early to earliest middle Miocene. The main part of the
- 220 Kadonosawa Formation has yielded abundant molluskan fossils (Chinzei, 1966), as well as a
- 221 tooth of *Desmostylus* (Oishi & Kawakami, 1984). Based on ostracods (Irizuki & Matsubara,
- 222 1994) and benthic foraminifera (Kamemaru, Matsubara & Irizuki, 1995), the depositional
- 223 environment of the Shikonai Siltstone Member of the Kadonosawa Formation conforms to
- 224 sublittoral to bathyal settings.

227

DESCRIPTION

Cranium

The cranium lacks most of the rostrum (Fig. 3), and the left orbit and parts of the left and right

- squamosal are also missing. In ventral view, the cranium has been dorsoventrally crushed in the
- area of the choanae. The choanae are cracked and not connected with the bony nares, anteriorly
- 231 depressed by secondary deformation (Fig. 4). In dorsal view, the nasals and the premaxillae are
- almost symmetrical, while the midline of the occipital condyle is slightly skewed to the right.
- 233 The cranium underwent some degree of oblique deformation, from the upper right to the lower
- 234 left and the dorsal part of the cranium might fall left by this deformation. In lateral view, the
- 235 temporal fossa is anteroposteriorly long and dorsoventrally high. The vertex is low and flat,
- being formed by the frontals and the nasals.

237238

Premaxilla

- The premaxillae are symmetrical. Most of the rostral portion of premaxillae is broken away. The broken section is just anterior to the antorbital notch. The premaxillary foramen is just posterior
- 241 to the broken section, and at the same level as the antorbital notch. Anteromedial to the
- premaxillary foramen, the anteromedial sulcus and the prenarial triangle are not preserved. No
- posteromedial sulcus of the premaxilla was observed. The lateral margin of each side of the
- premaxilla is also broken, and only remaining a recognizable premaxillary surface on right side
- of the maxilla. Anterior to the bony nares, the premaxillae are thin and flat. The posterolateral
- sulcus cannot be recognized, and the premaxillary sac fossa is weekly depressed. In lateral view,
- 247 the ascending process of the premaxillae form an angle of about 20° from the anteroposterior
- 248 axis of the cranium (Fig. 5). The knob-like posterior end of the premaxilla contacts the
- anterolateral corner of the nasal at a level slightly lower than the vertex of the cranium.

250251

Maxilla

- 252 The left maxilla is broken laterally, but the right antorbital notch is preserved. The maxillary-
- 253 palatine suture and the cross-section of the infraorbital canal are observed along the broken
- section (Fig. 6). The maxilla is generally flat transversely in the antorbital region, and there is no
- 255 indication that any maxillary crest was present. The lateral margin of the maxilla is flat in its
- orbital area, whereas it is slightly concave dorsally and posteriorly to the orbit. There are three
- anterior and one posterior dorsal infraorbital foramina on the right maxilla (Fig. 3). The



anteriormost of these foramina is located just besides the maxilla-premaxilla suture, anteromedial to the antorbital notch, other small anterior dorsal infraorbital foramina are located at the level of the orbit. The posterior dorsal infraorbital foramen is the largest, and its opening is located on the ascending process at the anteroposterior level of the corresponding nasal. The maxilla rises towards the vertex, gently at the ascending process but steeply along the lateral face of the vertex. Although the vertex is low, the maxilla faces laterally just lateral to the nasal and makes a pair of deep fossae intently medially by the nasal and posteriorly by the nuchal crest. In dorsal view, the posterior and lateral margins of the right maxilla are semicircular, and the posteromedial margin contacts the supraoccipital. In lateral view, the maxilla forms a thin plate and covers the frontal dorsally. It gradually thickens anteriorly at the antorbital process. In ventral view, the right ventral infraorbital foramen is preserved, while the lateral edge of the left ventral infraorbital foramen is broken away. The dorsolateral edge of the opening of the ventral infraorbital foramen is formed by the maxilla and the lacrimal or the jugal.

Palatine and Pterygoid

The posterior halves of both the palatines are preserved. The palatine-maxilla suture is visible from the anterior side through the broken transverse section of the rostrum base (Fig. 6). The palatine contacts the maxilla dorsally and is dorsoventrally thinner than the maxilla. The left and right palatines are not separated medially at the level of the transverse section, just anterior to the antorbital notch. The left side of the palatine is broken laterally, but the parasagittal section of the left infraorbital canal is observed (Fig. 4). The palatine-maxilla suture is not clear in the parasagittal section, and the ventromedial edge of the ventral infraorbital foramen is uncertain.

The pterygoids are well preserved, including both the lateral and ventral laminae of the pterygoid and the pterygoid hamuli. The anterior tip of the pterygoid is located slightly posteriorly to the level of the antorbital notch. The pterygoid sinus is ventrally covered by the pterygoid. The anterior edge of the pterygoid sinus is at the level of the antorbital notch. The palatal surface of the pterygoid is flat and ventrally convex. The sagittal portion of the two palatines do not contact each other medially in their posterior portion. The pterygoid hamulus is short and preserving the hamular crest. The hamular crests of the pterygoid diverges posteriorly in ventral view, extends to the posterolateral most of the lateral and ventral laminae of the pterygoid, just posterior to the infratemporal crest of the frontal. The medial lamina forms the anterolateral wall of the internal nares. Although the pterygoid-basioccipital is not preserved clearly, the posterior lamina overlaps the basioccipital crest. It forms the pharyngeal crest and covers the alisphenoid ventrally.

Vomer

The vomer is visible dorsally. When viewed from the anterior transverse section (Fig. 6), the premaxilla does not roof the vomer dorsally. The mesorostal groove is opened widely as a U-shaped groove, starting 11 mm anterior to the anterior edge of the bony nares. In ventral view, the vomer is covered by the pterygoid ventrally at the level of the choanae. It does not seem to



make contact with its posterior part since the deformation. It twists left and ventral to the posterior part (Fig. 6). The posterior part of the vomer is posteriorly overhung beneath the basisphenoid.

Presphenoid

The nasal septum is narrow transversely and straight dorsally. It is as high as the level of the nasal process of the premaxilla and posteriorly contacts both the nasals. Because of this, the cribriform plate cannot be distinguished in dorsal view.

Nasal

The shape of the nasal in dorsal view is subtriangular, and its transverse width is greater than its anteroposterior length. The left and right nasals are symmetrical. The nasal is slightly wider than the widest part of the bony nares, forms an approximate triangular bone with a posteriorly directed tip, slightly wider than its anterior margin. The lateral margin contacts the posterior end of the premaxilla anterolaterally and contacts the maxilla laterally. The nasals also contact the frontals posteromedially. The dorsal surface of the nasal is flat except for the slightly concave anterolateral part. There is no indication of an internasal fossa and the internasal suture is a shallow trough. In dorsal view, the anterior border of the nasal is slightly retracted posteriorly from the bony nares.

Frontal

The frontal is only exposed dorsally at the vertex. In dorsal view, the frontal is separated from the maxilla by the nasal. The dorsal exposure of the joined frontals on the vertex is elliptical, and it contacts the nasal anterolaterally and the supraoccipital posteriorly, but not contacting with the maxilla laterally. The frontal at the vertex is slightly higher than the nasal, being the highest point of the cranium. In lateral view, the orbit seems markedly concave and low, in line with the lateral edge of the posterior part of the rostrum (Fig. 5). In lateral view, the preorbital process is thick anteriorly. While the anteriormost part of the frontal is broken, the frontal-lacrimal suture is not clear. Although its broken the postorbital process, is somewhat transversely narrow and triangular at the base, being directed posteroventrally or ventrally. Both the fossae for the preorbital and the postorbital lobes of the pterygoid sinus are shallow or absent. The frontal groove is deep medially, extant anteriorly to the level of the ventral infraorbital foramen. The infratemporal crest is curved, distinct just lateral to the optic canal.

Lacrimojugal Complex

The left antorbital process is broken, and the right antorbital process is also broken anteriorly and laterally, so that the shape and the anteriormost portion of the antorbital process is not clear. Although both the lacrimal-maxilla suture and the lacrimal-jugal suture are not clear in dorsal view, the lacrimal-maxilla suture might be observable in anterior view along the broken section of the antorbital process. Here the lacrimal appears as thicker than the maxilla. The right jugal



contacts the lacrimal exactly at the posterior end of the antorbital notch. The main part of the right jugal is broken, only preserved as a short narrow base of the maxillary process.

Squamosal

The right squamosal is almost missing, while the anterior part of the glenoid process of the left squamosal is preserved as a short base, missing the squamosal fossa and the zygomatic process. The glenoid process might have been long because the postorbital process is relatively far from the base of the glenoid process. The squamosal fossa is incomplete anteriorly, but it is shallow and somehow longer anteroposteriorly and transversely wide, and it faces dorsally. The lateral margin of the fossa is visible in dorsal view. The mandibular fossa is not preserved, while the tympanosquamosal recess can be observed medially. The tympanosquamosal recess is flat and wide, and its ventral surface is wrinkled. The falciform process is not well preserved. The dorsal roof of the external auditory meatus is preserved and is distinctively narrow, but the postglenoid process just in front of the external auditory meatus is not clear because of insufficient preservation. The retrotympanic process is not preserved.

Supraoccipital

The supraoccipital is broadly exposed in dorsal view. The nuchal crest is trapezoidal in outline, while it is medially concave at the level of the temporal fossa. It expands laterally toward to the exoccipital. In posterior view, the supraoccipital is inclined anteriorly with a reduced dorsoventral height. The occipital shield is concave anterodorsally and convex posteroventrally. Anteromedially, just posterior to the nuchal crest, the supraoccipital concaves dorsally, forms a fossa whose anterior most surface faces posteriorly. Posteriorly, the occipital shield bulges medially, posterior to the nuchal crest (Fig. 7) and it is collapsed along the right margin, this sounds very likely be a result of deformation. The supraoccipital is fused with the exoccipital along an undefined suture. There is no indication of an external occipital crest.

Exoccipital

The exoccipital is wide in posterior view. It extends laterally from the temporal crest and is fused with the basioccipital ventrally. The temporal crest overhangs the exoccipital posterolaterally, and extants nearly to the posterior most level of the cranium not taking account of the condyles. The occipital condyle is prominent, and the condylar neck is well developed, while there is no indication of a dorsal condyloid fossa. The foramen magnum is almost circular, being only slightly higher than wide. In posterior view, the jugular notch is deep and narrow. The paroccipital process is wide. The hypoglossal foramen is opened at the jugular notch. The paroccipital concavity is deep and it is separated from the jugular notch by the paroccipital process.

Basioccipital



The basioccipital basin is broad and strongly concave in posterior view. The basioccipital crests face ventromedially at their margins. In ventral view, the basioccipital width is transversely 378 narrow, just posteriorly expands slightly than anteriorly. It contacts with the posterior lamina of 379 the pterygoid. Its posterior margin is rounded. Medial to the crest, the ventral surface of the basioccipital is flat. The muscular tubercle is not developed on the basioccipital basin.

381 382 383

384

385

386

387

388

389 390

391

392

393 394

395

396

397

398

399

400

401

402 403

404

405

406 407

408

409

410 411

380

377

Periotic

The right periotic is preserved (Figs. 8 and 9). In dorsal and ventral views, the apex of the anterior process is mediolaterally flattened. Both anteroventral and anterodorsal angles are respectively tapered and directed anteriorly, reaching the same level anteriorly and preserved the anterior keel. The anteroposterior length of the anterior process is nearly the same as that of the pars cochlearis. The anterior incisure is deep, and it separates the anterior process from the pars cochlearis. In lateral view, the ventral surface of the parabullary ridge is concave. There is a flat surface anterior to the fovea epitubaria, which is circular and about 2 mm long, which might correspond to a very shallow anterior bullar facet. The fovea epitubaria is broad, and it receives with no fusion the accessory ossicle of the tympanic bulla. There is a fossa posteromedial to the fovea epitubaria and anteromedial to the mallear fossa. It receives the tubercle of the malleus. The mallear fossa is rounded and faces ventrally rather than medially. The lateral tuberosity is bulbous lateral to the mallear fossa. The epitympanic hiatus is concave just posterior to the lateral tuberosity. The hiatus accommodates the facial canal posteromedially. The vestibular window is rounded and slightly larger than the opening for the facial canal.

The medial outline of the pars cochlearis is rounded and compressed dorsoventrally. The cochlear window opens on the posterior wall of the pars cochlearis. The aperture for the cochlear aqueduct opens dorsally and is located close to the vestibular aqueduct at the same transverse level as the medial edge of the internal acoustic meatus. The aperture for the vestibular aqueduct is two times larger than the aperture for the cochlear aqueduct and located slightly posteriorly to the aperture for the cochlear aqueduct. The internal acoustic meatus is large and funnel-shaped, with an anterolateral—posteromedial axis. The anterior most tip of the internal acoustic meatus extends in the anterior incisure. The foramen singulare is located closer to the proximal opening of the facial canal than to the spiral cribiform tract, and it is separated by partitions from the proximal opening of the facial canal and the spiral cribiform tract. The proximal opening of the facial canal is located slightly anterior to the spiral cribriform tract. The area cribrosa media has almost the same size as the spiral cribriform tract. The posterior process extends for a short distance anteroventrally, while its posterior edge is directed ventrally. In lateral view, the posterior and dorsal faces of the posterior process draw a blunt right angle. The posterior bullar facet is smooth and faces anteroventrally.

412 413 414

Tympanic bulla

415 The right tympanic bulla only lacks the anterodorsal crest (Figs. 10 and 11). The accessory 416 ossicle is preserved but detached from the tympanic bulla. The tympanic bulla is narrow and long



in lateral view, and its ventral margin is slightly concave in lateral view. The lateral furrow is absent or very shallow. The disarticulated accessory ossicle is rounded, 8.3 mm in width. It originally occupied the fovea epitubaria of the periotic. In ventral view, there is an antero-posterior linear fracture surface on the accessory ossicle, for the attachment to the outer lip of the tympanic. The involucrum tapers anteriorly, and the anterior spine is absent. The dorsal and ventral margins of the involucrum are parallel and the dorsal margin is excavated just anterior to the posterior process. The ventromedial keel on the involucrum is not clearly defined. The interprominential notch is shallow and is followed anteriorly by the median furrow. The median furrow is shallow. It widens anteriorly and points laterally. In dorsal view, the sigmoid process is large and rounded, and it partly covers the conical process. The posterior edge of the sigmoid process is thick. The conical process is dorsally high. The inner and outer posterior prominences extend posteriorly to the same level, and they are almost equal in transverse width. The posterior process, which is broken at its base, is rounded in outline and thick. The facet for the posterior process of the periotic is smooth. The elliptical foramen can be observed between the outer and inner posterior pedicles.

Malleus

The malleus is isolated from the periotic (Fig. 12 A–F). The head is high anteromedially. The ventral margin of the tubercle is concave. The manubrium of the malleus forms a hook-like process at the medial margin, which directs anteriorly. The insertion for the tendon of the m. tensor tympani opens ventrally. The processus muscularis is small.

Mandible

Both the left and right mandibles are partly preserved (Fig. 12 K–N), but the right mandible only preserves its posterior part, while the left mandible preserves its posteroventral part including the angular process and the ventral half of the mandibular condyle. The mandibular foramen is shallow mediolaterally. The left mandible does not preserve the anterior margin of the mandibular foramen. The posterior margin of the angular process is rounded, and the medial surface is concave. The mandibular condyle is located more posteriorly than the angular process and is separated from the latter by an anteriorly inward, deep, rounded curve that connects it with the angular process and the mandibular condyle. The medial surface of the condyle is concave and the condylar articular surface is not preserved.

Tooth

One isolated tooth is preserved (Fig. 12 G–J). It is small and conical, at least 27 mm long and with a maximum diameter of the root of 6.3 mm. The crown surface is smooth and its apex is curved. The tooth root is also smooth and conical, and it is 1.5 times longer than the crown. The cementum of the root is just slightly thicker than the crown, and the tip of the root is recurved in a direction that is at right angle with the curve of the crown's apex.



Vertebra

Only a fragment of the atlas is preserved (Fig. 12 O, P). The ventral part of the bone, without the upper transverse processes is preserved. In posterior view, the posterior articular surface is not well preserved, but it was originally not fused with the axis. In dorsal view, the anterior tubercle is short anteroposteriorly and relatively high dorsoventrally. It bears a V-shaped crest on its anterior surface, starting from the ventral most of the anterior articular facet and runs the ventral apex of the anterior tubercle.

Results of Phylogenetic Analyses

Our phylogenetic analysis found 256 most parsimonious trees with 3424 steps of total branch length. Each tree has a consistency index of 0.197 and a retention index of 0.564. The 50% majority rule consensus of those trees is shown in Figure 13, and the strict consensus tree is shown in the Figure 14 (see also Supplemental Information). Both consensus trees show that all the species that were previously identified as kentriodontids are nested in a monophyletic group that is positioned as the sister group to the crown Delphinoidea (i.e., Delphinidae, Phocoenidae and Monodontidae), and the clade Lipotidae + Inioidea is basal to the clade Delphinoidea (monophyletic Kentriodontidae + crown Delphinoidea).

The Delphinoidea is deferent from Lipotidae + Inioidea by the following 11 synapomorphies: The anterior sinus fossa is located between the anterior extremity of the pterygoid sinus and the posterior extremity of the upper tooth row (Chr. 19), the apex of the postorbital process of frontal is directed ventrally (Chr. 61), the width of the premaxillae at the antorbital notches is moderate (Chr. 67), the apex of the anterior process of the periotic is thickened by the prominent dorsal tubercle that gives to this apex a rectangular section on the plane of the body of the periotic (Chr. 239), the contact of the anterior process of the petrosal with a portion of the ectotympanic bulla anterior to the accessory ossicle is absent (Chr. 249), the periotic articulates with the squamosal along the hiatus epitympanicus and adjacent regions on the posterior process (Chr. 286), length of the posterior process of the periotic is long (Chr. 292), lateral furrow of the tympanic bulla present as a shallow groove (Chr. 303), and the ventral margin of the tympanic bulla concave in lateral view (Chr. 307), the basihyal and the thyrohyal is fused (Chr. 322), and the roof of the neural canal of the atlas is straight (Chr. 327).

The monophyly of Kentriodontidae is supported by the following 14 synapomorphies: premaxillae are compressed mediolaterally at anterior of the rostrum (Chr. 3), the mesorostral groove is constricted posteriorly, anterior to the nares and behind the level of the antorbital notch, then rapidly diverging anteriorly (Chr. 7), anterior edge of the supraorbital process is oriented anterolaterally, forming angle with the longitudinal axis of the skull between 35° and 60° (Chr. 50), the dorsolateral edge of internal opening of the infraorbital foramen is formed by the lacrimal or the jugal (Chr. 58), the infratemporal crest forms well-defined curved ridge on the posterior edge of sulcus for the optic nerve (Chr. 64), the premaxillary foramen is located medially (Chr. 72), the alisphenoid is broadly exposed laterally in the temporal fossa (Chr. 160), suture between the joined palatines and the joined maxillae is straight transversely or bowed



anteriorly (Chr. 179), the external auditory meatus is wide (Chr. 225), angle formed by basioccipital crests as approximately 15–40° in ventral view (Chr. 229), the hypoglossal foramen is separated from the jugular foramen or the jugular notch by thick bone (Chr. 231), most convex part of the pars cochlearis is on the ventrolateral surface (Chr. 283), the basihyal fused with the thyrohyal (Chr. 332), and the lateral edge of transverse processes of lumbar vertebrae makes an angle of 45° or more relative to the parasagittal plane (Chr. 334). However, the last two characters (i.e., Chrs. 332 and 334) are not known for most kentriodontid taxa.

The monophyly of the genus *kentriodon* was recognized by five unique characters as was mentioned in the generic diagnosis. In particular, '*Rudicetus*' squalodontoides was recognized as a sister taxon to *Kentriodon diusinus* and consequently bracketed among the species of the latter genus. NMHF 999 was also nested in the genus *Kentriodon* and recognized as a sister taxon to the clade of *K. pernix*, *K. nakajimai* and *K. obscurus* (Fig. 13).

Comparison

Like most of kentriodontids, the premaxillae and nasals of NMHF 999 are symmetrical. Also, the vertex of NMHF 999 is low and flat, similar to most species of *Kentriodon*. Unlike the condition in K. hobetsu, K. pernix and K. schneideri, the maxilla of NMHF 999 makes a pair of deep fossae and faces laterally at the vertex, intently medially by the nasal and posteriorly by the nuchal crest. This feature is similar to K. nakajimai and some other genera of kentriodontids such as D. dividum, H. calvertense, L. pappus, L. calvertensis, L. repenningi and M. morani. The nasal septum of NMHF 999 is high, as high as the same level of the nasal process of the premaxilla. This feature is unique to NMHF 999 and unlike other *Kentriodon* nor other genera of kentriodontids. In dorsal view, the nasal of NMHF 999 is similar with that in K. pernix, D. dividum and T. joneti. However, the condition is different from that in K. pernix and D. dividum, but similar as in T. joneti, the nasal of NMHF 999 posteriorly extends to the nuchal crest, and the frontal is somewhat not contacting with the maxilla laterally. The supraoccipital of NMHF 999 is concave dorsally and anteriorly, just posterior to the line of the nuchal crest at the vertex. It is similar with the condition in K. nakajimai, K. schneideri, also in R. squalodontoide, but different from some other Kentiodon such as K. pernix and K. hobetsu. In dorsal view, the supraoccipital shield of NMHF 999 is convex posteriorly as in K. pernix. Although this feature may be emphasized by deformation on NMHF 999, the same portion is straight posteriorly in most of Kentriodon. In ventral view, the tympanosquamosal recess of NMHF 999 is flat and wide. similar to that in K. pernix and K. hobetsu, while this feature is not preserved clearly in most of Kentriodon.

The apex of the anterior process of the periotic of NMHF 999 is directed anteriorly in dorsal views, and the anteroposterior length of the anterior process is as long as the length of the pars cochlearis. These conditions are similar with those in *H. calvertense*, *W. chinookensis*, *Liolithax kernensis* and *L. pappus*. In contrast, in *K. nakajimai*, *K. obscurus*, *K. hoepfneri* and *K. pernix*, the apex of the anterior process of the periotic is somewhat directed anteromedially, and the anterior process of the periotic is shorter than the length of the pars cochlearis. In NMHF



537 999, the lateral tuberosity of the periotic is ventrally as high as that in K. nakajimai and K. pernix, but it is higher than that in K. hoepfneri and other genera of kentriodontids (i.e., L. 538 pappus, W. chinookensis, K. serrulus and Sophianacetus commenticius). In dorsal view, the 539 anterolateral margin of the pars cochlearis is separated from the anterior process by the deep 540 541 facial canal in NMHF 999. This feature is also observed in K. pernix, L. kernensis and W. chinookensis. The interprominental notch of the tympanic bulla in NMHF 999 is shallow as in D. 542 dividum K. serrulus and W. chinookensis, while this notch is much deeper in A. iquensis, K. 543 nakajima, K. pernix, and S. commenticius. 544

Based on our phylogenetic analysis and those comparisons, identification of NMMF 999 as a distinct species within the genus *Kentriodon* is warranted. Thus, we propose *Kentriodon* sugawarai sp. nov.

547 548 549

550

566

567

568

569 570

571

575

576

545

546

Discussion and Conclusions

Phylogenetic Position of the Kentriodontids

- Our analysis suggests that all the species of kentriodontids form a monophyletic group. Although 551
- the monophyly of the kentriodontids has been proposed in some earlier studies (e.g., Barnes, 552
- 1978, 1985; Muizon, 1988a), the intergeneric and interspecific therein proposed for the members 553
- 554 of this family are both different from our results (fig. 1). Here we suggest that kentriodontids are
- 555 divided into two monophyletic subgroups (fig. 13). The first subgroup includes Kampholophos,
- Wimahl, 'Rudicetus', and Kentriodon, while the second subgroup includes Delphinodon, 556
- Tagicetus, Macrokentriodon, Liolithax, Hadrodelphis, Pithanodelphis, Lophocetus, and 557
- Atocetus. The 50% majority rule consensus tree (fig. 13) shows agreements with Lambert et al. 558
- (2017), Peredo, Uhen & Nelson (2018) and Kimura & Hasegawa (2019) at least as regards the 559
- 560 former subgroup (fig. 1). In this regard, the monophyly of the former subgroup is considered to
- be robust. On the other hand, other kentriodontids had been subdivided into five paraphyletic or 561
- polyphyletic groups by Lambert et al. (2017) and Peredo, Uhen & Nelson (2018). Particularly, 562
- 563 both of their unconstrained analysis suggested that a kentriodontid species *Liolithax* was
- 564 recognized as a sister taxon to the Lipotidae, meaning that it was recognized to be more closely 565 related to Iniidae + Pontoporiidae than other 'kentriodontids'.

Particularly, the result of our phylogenetic analysis is somewhat similar to that obtained by Tanaka et al. (2017), but the interrelationships of the Delphinida (Lipotidae + Inioidea + Kentriodontidae, as redefined herein + crown Delphinoidea) are different in the two studies (fig. 1). As regards Delphinida, the interrelationships of the crown Delphinoidea (Delphinidae + Monodontidae + Phocoenidae), including the extinct taxa, also recall those recovered by Tanaka et al. (2017), but the sister group relationships among Delphinida (Lipotidae + Inioidea + Kentriodontidae) are different. Tanaka et al. (2017) included in their analysis only three

572

kentriodontids and suggested that they formed a paraphyletic group. These three kentriodontids 573 were located basal to the crown Delphinoidea. 574

As mentioned above, we performed our phylogenetic analysis by applying a tree constraint based on molecular evidence by McGowen, Spaulding & Gatesy (2009), McGowen et



593

594

595

596 597

598 599

600

601

602 603

604

605

606 607

608

609

610

611

612

613

614 615

616

577 al. (2011) and McGowen et al. (2020) (fig. 1) as was also the case for the analysis by Tanaka et al. (2017). Lambert et al. (2017) performed their phylogenetic analyses both with a tree 578 constraint based on molecular evidence and without such a tree constraint, and they preferred 579 their unconstrained tree as a result from their multiple analyses. The study by Lambert et al. 580 581 (2017) was so comprehensive that it might be the reason why the molecular evidence had not been used in later studies on the phylogeny of the Delphinida including the kentriodontids (e.g., 582 Peredo, Uhen & Nelson, 2018; Kimura & Hasegawa, 2019, 2020). Molecular phylogenetics is 583 now widely accepted for reconstructing the phylogenetic relationships of organisms, but its 584 results are sometimes different from analyses based only on morphological data. Although many 585 of those studies aforementioned (e.g., Lambert et al., 2017; Peredo, Uhen & Nelson, 2018; 586 Kimura & Hasegawa, 2019) chose the total evidence approach (parsimony analysis based both 587 on molecular and morphological evidence) for their analyses, the resulting relationships they 588 589 suggested are different from that of the analyses based on molecular data only in regard to the 590 extant species (McGowen, Spaulding & Gatesy, 2009; McGowen et al., 2011; McGowen et al., 2020; Geisler et al., 2011; Lambert et al., 2020). 591

Because of relatively low bootstrap values for the result of our phylogenetic analysis, the morphological evidence for the monophyly of kentriodontids are still not robust in support. But, it should be emphasized that the result of our parsimony analysis with tree constraint by molecular evidence is consequently no contradiction with molecular phylogenetics for the extant species for the first time.

Diversifications of Delphinida Based on the Ear Bones

At the time of the evolution and diversification of delphinidans, including Lipotidae, Inioidea, monophyletic kentriodontids, and crown Delphinoidea, the seven out of 18 synapomorphies are considered as evolutionary changes of periotic and tympanic bulla features. These changes could be interpreted to be the result of their evolutionary innovation such as the potential specialization of their echolocation abilities among odontocetes (Gutstein et al., 2014; Churchill et al., 2016). These characters are the following: the processus muscularis of the malleus is sub-equal or longer than the manubrium (Chr. 237), the articulation of the anterior process of the periotic with the squamosal is absent (Chr. 253), the anterior bullar facet is absent (Chr. 254), the dorsal surface of the periotic is nearly flat (Chr. 260), the foramen singulare forms a shared recess with the spiral cribiform tract, the transverse crest that separates it from the proximal opening of the facial nerve canal is low, and the proximal opening of the facial nerve canal is within the internal acoustic meatus (Chr. 269), the aperture for the cochlear aqueduct is smaller than the aperture for the vestibular aqueduct (Chr. 272), and the dorsal margin of the involucrum of the tympanic bulla is excavated just anterior to the posterior process (Chr. 317). Furthermore, the node uniting the kentriodontids and the crown delphinoids is supported by 11 synapomorphies, additional six of which regard the auditory specializations, namely: the apex of the anterior process of the periotic is thickened by the prominent dorsal tubercle that gives to this apex a rectangular section on the plane of the body of the periotic (Chr. 239), the contact of the anterior process of the



petrosal with a portion of the ectotympanic bulla anterior to the accessory ossicle is absent (Chr. 617 249), the periotic articulates with the squamosal along the hiatus epitympanicus and adjacent 618 regions on the posterior process (Chr. 286), length of the posterior process of the periotic is long 619 (Chr. 292), lateral furrow of the tympanic bulla present as a shallow groove (Chr. 303), and the 620 621 ventral margin of the tympanic bulla concave in lateral view (Chr. 307). Compared with other odontocetes, the ear bones of delphinidans are highly specialized (e.g., Fraser & Purves, 1960; 622 Gutstein et al., 2014), and kentriodontids share a number of tympanoperiotic apomorphies with 623 the crown delphinoids rather than with those of inioids (see also Gutstein et al., 2014). These 624 morphological changes of the periotic and tympanic bulla in the Delphinida are thought to have 625 626 been emphasized by their diversification or specialization of functional relationships between the periotic, tympanic bulla, and nearby portion of the skull during the process of the acquisition of 627 much higher frequency (i.e., ultrasonic) sound hearing abilities (e.g., Gutstein et al., 2014; Ary, 628 629 2017), and sound reception mechanism (Cranford, Krysl & Amundin, 2010). These changes 630 might also have allowed delphinidans to diversify their abilities of echolocation, such as narrowband and bimodal sound structure (e.g., Churchill et al., 2016; Mourlam & Orliac, 2017) and 631 habitat preferences (Costeur et al., 2018). However, the direct relationship of the above structural 632 changes of tympanoperiotics and resulting functional innovations are still uncertain (Gutstein et 633 al., 2014), and the whole characters mentioned above have not been confirmed sufficiently for 634 the influences with the specialization of hearing. Therefore, relationships between these 635 morphological and functional changes should be proved through further work. Nevertheless, 13 636 tympanoperiotic characters out of 29 characters as synapomorphies for the Delphinida still 637 indicate their specialization and innovation of hearing abilities. 638

639 The kentriodontids exhibited high diversity among the delphinidans during the Miocene (Ichishima et al., 1995, Marx, Lambert & Uhen, 2016, Plate 16a). Based on published records 640 (Ichishima et al., 1995; Ichishima, 1995; Dawson, 1996a; Dawson, 1996b; Bianucci, 2001; 641 Kazár, 2005; Kazár & Grigorescu, 2005; Lambert, Estevens & Smith, 2005; Kazár, 2006; 642 643 Whitmore & Kaltenbach, 2008; Kazár & Hampe, 2014; Salinas-Márquez et al., 2014; Peredo, Uhen & Nelson, 2018; Kimura & Hasegawa, 2019), all 31 taxa that can be recognized to be 644 kentriodontids are known in the Miocene; 6 taxa in the early Miocene, 19 taxa in the middle 645 Miocene and 6 taxa in the late Miocene, respectively. Conversely, the crown delphinoids and the 646 647 inioids almost never appeared until the end of the middle Miocene. In this regard, the kentriodontids was geochronologically a first independent and diverse group within the 648 delphinidans, and they were a unique group with consecutive modifications of ear bones within 649 the odontocetes. Since the high ratio of the morphological changes observed in their 650 tympanoperiotics and their high species richness, the innovation with specializations of their 651 hearing apparatus in kentriodontids probably resulted in their great diversification during the 652 period between the early and middle Miocene. 653

Institutional abbreviations

654 655

656

NMHF Ninohe Museum of History and Folklore, Ninohe City, Iwate, Japan.



657	NMNS-PV	Fossil vertebrate collections at the National Museum of Nature and Science,	
658		Tsukuba, Japan.	
659	NSMT-M	Marine mammal collections at the National Museum of Nature and Science,	
660		Tsukuba, Japan.	
661			
662	Acknowledgements		
663	We wish to thank K. Sugawara (then NMHF), Y. Seki (NMHF) and Y. Inaba (NMHF)		
664	for permitting us to describe NMHF 999. We also thank Y. Tajima (NMNS), T. Kimura		
665	(GMNH) for providing access to the collections under their care. Our thanks also go to Y.		
666	Tajima and T.K. Yamada (NMNS), M. Oishi (then Iwate Prefectural Museum), H. Ichishima		
667	(Fukui Prefectural Dinosaur Museum) and Y. Yanagisawa (Geological Survey of Japan) for		
668	providing useful discussion and advice. We appreciate K. Sashida (then University of Tsukuba,		
669	now Mahidol Univ.) and S. Agematsu (Univ. Tsukuba) for their help during field works. We are		
670	grateful to K. Sashida, S. Agematsu, K. Tanaka (Univ. Tsukuba), and Yasunari Shigeta		
671	(NMNS/Univ. Tsukuba) for their useful advice, discussion and generous encouragement during		
672	the course of this study. The manuscript has been greatly improved by careful attention to detail		
673	and extensive comments from PeerJ editor H. Brando, reviewers N. Pyenson, O. Lambert and an		
674	anonymous r	eviewer. We appreciate their efforts very much.	
675			
676	Reference	es	
677	Ary WJ. 2017. Form, function and phylogeny in the cetacean ear complex. San Diego State		
678	University, ProQuest Dissertations Publishing 10689605.		
679	Barnes LG. 1	978. A review of Lophocetus and Liolithax and their relationships to the delphinoid	
680	family k	Kentriodontidae (Cetacea: Odontoceti). Bulletin of the Natural History Museum of	
681	Los Ang	seles County 28:1–35.	
682	Barnes LG. 1	985. The Late Miocene dolphin <i>Pithanodelphis</i> Abel, 1905 (Cetacea-	
683	Kentrio	dontidae) from California.pdf. Contributions in Science:1–27.	
684	Barnes LG, N	Mitchell ED. 1984. Kentriodon obscurus (Kellogg, 1931), a fossil dolphin	
685	(Mamm	alia: Kentriodontidae) from the Miocene Sharktooth Hill Bonebed in California.	
686	Contrib	utions in Science (Los Angeles) 353:1–23.	
687		2001. A new genus of kentriodontid (cetacea: Odontoceti) from the miocene of	
688		aly. Journal of Vertebrate Paleontology 21:573–577. DOI: 10.1671/0272-	
689	4634(20	001)021[0573:ANGOKC]2.0.CO;2.	
690	Chinzei K. 19	966. Younger Tertiary geology of the Mabechi River valley, northeast Honshu,	
691	Japan. Journal of the Faculty of Science, the University of Tokyo. Sect. II 16:161–208.		
692	Churchill M, Martinez-Caceres M, de Muizon C, Mnieckowski J, Geisler JH. 2016. The Origin		
693	of High-Frequency Hearing in Whales. Current Biology 26:2144–2149. DOI:		
694	10.1016	/j.cub.2016.06.004.	



- Cope ED. 1867. An Addition to the Vertebrate fauna of the Miocene Period, with a Synopsis of
 the Extinct Cetacea of the United States. *Proceedings of the Academy of Natural Sciences of Philidelphia* 19:138–156.
- Costeur L, Grohé C, Aguirre-Fernández G, Ekdale E, Schulz G, Müller B, Mennecart B. 2018.
 The bony labyrinth of toothed whales reflects both phylogeny and habitat preferences.
 Scientific Reports 8. DOI: 10.1038/s41598-018-26094-0.
- Cranford TW, Krysl P, Amundin M. 2010. A new acoustic portal into the odontocete ear and vibrational analysis of the tympanoperiotic complex. *PLoS ONE* 5. DOI:
 10.1371/journal.pone.0011927.
- Dawson SD. 1996a. A description of the skull and postcrania of *hadrodelphis calvertense* kellogg 1966, and its position within the kentriodontidae (cetacea; delphinoidea). *Journal of Vertebrate Paleontology* 16:125–134. DOI: 10.1080/02724634.1996.10011290
- Dawson SD. 1996b. A new kentriodontid dolphin (cetacea; delphinoidea) from the middle
 miocene choptank formation, Maryland. *Journal of Vertebrate Paleontology* 16:135–140.
 DOI: 10.1080/02724634.1996.10011291.
- Flower WH. 1872. On the recent Ziphioid whales, with a Description of the Skeleton of
 Berardius arnouxi. The Transactions of the Zoological Society of London 8:203–234. DOI:
 10.1111/j.1469-7998.1872.tb08572.x.
- Fraser FC, Purves PE. 1960. Hearing in Cetaceans. Evolution of the accessory air sacs and the structure and function of the outer and middle ear in recent cetaceans. *Bulletin of the British Museum (Natural History) Zoology* 7:1–140, 53 pls. frontis.
- Gatesy J, Geisler JH, Chang J, Buell C, Berta A, Meredith RW, Springer MS, McGowen MR.
 2013. A phylogenetic blueprint for a modern whale. *Molecular Phylogenetics and Evolution* 66:479–506. DOI: 10.1016/j.ympev.2012.10.012.
- Geisler JH, Godfrey SJ, Lambert O. 2012. A new genus and species of late Miocene inioid
 (Cetacea, Odontoceti) from the Meherrin River, North Carolina, U.S.A. *Journal of Vertebrate Paleontology* 32:198–211. DOI: 10.1080/02724634.2012.629016.
- Geisler JH, McGowen MR, Yang G, Gatesy J. 2011. A supermatrix analysis of genomic,
 morphological, and paleontological data from crown Cetacea. *BMC Evolutionary Biology* 11. DOI: 10.1186/1471-2148-11-112.
- Goloboff PA, Catalano SA. 2016. TNT version 1.5, including a full implementation of phylogenetic morphometrics. *Cladistics* 32:221-238. DOI: 10.1111/cla.12160
- Goloboff PA, Farris JS, Nixon KC. 2008. TNT, a free program for phylogenetic analysis.
 Cladistics 24:774–786. DOI: 10.1111/j.1096-0031.2008.00217.x.
- 729 Gutstein CS, Figueroa-Bravo CP, Pyenson ND, Yury-Yañez RE, Cozzuol MA, Canals M. 2014.
- High frequency echolocation, ear morphology, and the marine-freshwater transition: A
- comparative study of extant and extinct toothed whales. *Palaeogeography*,
- *Palaeoclimatology, Palaeoecology* 400:62–74. DOI: 10.1016/j.palaeo.2014.01.026.



- 733 Ichishima H. 1995. A new fossil kentriodontid dolphin (Cetacea; Kentriodontidae) from the
- Middle Miocene Takinone Formation, Hokkaido, Japan. *The Island Arc* 3, 473–485 (for
- 735 1994). DOI: 10.1111/j.1440-1738.1994.tb00126.x
- 736 Ichishima H, Barnes LG, Fordyce RE, Kimura M, Bohaska DJ. 1995. A review of kentriodontine
- dolphins (Cetacea; Deiphinoidea; Kentriodontidae): Systematics and biogeography. *Island*
- 738 *Arc* 3:486–492 (for 1994). DOI: 10.1111/j.1440-1738.1994.tb00127.x.
- 739 Ichishima H. 2016. The ethmoid and presphenoid of cetaceans. *Journal of Morphology* 277:1661–1674.
- 741 Irizuki T, Matsubara T. 1994. Vertical changes of depositional environments of the Lower to
- 742 Middle Miocene Kadonosawa Formation based on analyses of fossil ostracode faunas. *The*
- Journal of the Geological Society of Japan 100:136–149. [Japanese with English abstract]
- 744 Kamemaru A, Matsubara T, Irizuki T. 1995. Foraminiferal assemblage in the Lower to Middle
- Miocene Kadonosawa Formation at the type locality, Iwate Prefecture. *Abstract of the*
- 746 *102nd Annual Meeting of the Geological Society of Japan*:93. [Japanese]
- 747 Kazár E, Hampe O. 2014. A new species of *Kentriodon* (Mammalia, Odontoceti, Delphinoidea)
- from the middle/late Miocene of Groß Pampau (Schleswig-Holstein, North Germany).
- 749 *Journal of Vertebrate Paleontology* 34:1216–1230. DOI:10.1080/02724634.2014.85734
- Kazár E. 2005. A new kentriodontid (Cetacea: Delphinoidea) from the Middle Miocene of Hungary. *Fossil Record* 8:53–73. DOI:10.1002/mmng.200410004.
- 752 Kazár E. 2006. Odontocete periotics (Mammalia: Cetacea) from the Carpathian Basin, middle
- Miocene (Badenian and Sarmatian Stages), including the Vienna Basin, Austria. Beitrage zur Palaontologie 30:269–292.
- 755 Kazár E, Grigorescu D. 2005. Revision of Sarmatodelphis moldavicus Kirpichnikov, 1954
- (Cetacea: Delphinoidea), from the Miocene of Kishinev, Republic of Moldavia. *Journal of Vertebrate Paleontology* 25:929–935.
- Kellogg A. R. 1927. *Kentriodon pernix*, a Miocene porpoise from Maryland. *Proceedings of the United States National Museum* 69:1-55.
- Kellogg R. 1931. Pelagic Mammals from the Temblor Formation of the Kern River Region,
 California. *Proceedings of the California Academy of Sciences* XIX:217–397.
- 762 Kimura T, Hasegawa Y. 2019. A new species of *Kentriodon* (Cetacea, Odontoceti,
- Kentriodontidae) from the Miocene of Japan. *Journal of Vertebrate Paleontology* 39:1–14. DOI: 10.1080/02724634.2019.1566739.
- Kimura T, Hasegawa Y. 2020. *Norisdelphis annakaensis*, A new Miocene delphinid from Japan.
 Journal of Vertebrate Paleontology:e1762628. DOI: 10.1080/02724634.2020.1762628.
- 767 Lambert O, Bianucci G, Urbina M, Geisler JH. 2017. A new inioid (Cetacea, Odontoceti,
- Delphinida) from the Miocene of Peru and the origin of modern dolphin and porpoise
- families. Zoological Journal of the Linnean Society 179:919–946. DOI: 10.1111/zoj.12479.
- Tro Lambert O, Collareta A, Benites-Palomino A, Di Celma C, de Muizon C, Urbina M, Bianucci G.
- 771 2020. A new small, mesorostrine inioid (Cetacea, Odontoceti, Delphinida) from four upper

- Miocene localities in the Pisco Basin, Peru. *Papers in Palaeontology*:spp2.1332. DOI:
 10.1002/spp2.1332.
- Lambert O, Estevens M, Smith R. 2005. A new kentriodontine dolphin from the middle Miocene
 of Portugal. *Acta Palaeontologica Polonica* 50:239–248.
- Lambert O, Muizon C de, Malinverno E, Di Celma C, Urbina M, Bianucci G. 2018. A new
 odontocete (toothed cetacean) from the Early Miocene of Peru expands the morphological
 disparity of extinct heterodont dolphins. *Journal of Systematic Palaeontology* 16:981–1016.
 DOI: 10.1080/14772019.2017.1359689.
- Marx FG, Lambert O, Uhen MD. 2016. *Cetacean Paleobiology*, Wiley Blackwell, Topics in
 Paleobiology, 319. DOI:10.1002/9781118561546
- McGowen MR, Montgomery SH, Clark C, Gatesy J. 2011. Phylogeny and adaptive evolution of
 the brain-development gene microcephalin (MCPH1) in cetaceans. *BMC Evolutionary Biology* 11. DOI: 10.1186/1471-2148-11-98.
- McGowen MR, Spaulding M, Gatesy J. 2009. Divergence date estimation and a comprehensive molecular tree of extant cetaceans. *Molecular Phylogenetics and Evolution* 53:891–906.
 DOI: 10.1016/j.ympev.2009.08.018.
- McGowen MR, Tsagkogeorga G, Álvarez-Carretero S, Dos Reis M, Struebig M, Deaville R,
 Jepson PD, Jarman S, Polanowski A, Morin PA, Rossiter SJ. 2020. Phylogenomic
 Resolution of the Cetacean Tree of Life Using Target Sequence Capture. *Systematic* Biology 69:479–501. DOI: 10.1093/sysbio/syz068.
- Mead JG, Fordyce RE. 2009. The therian skull: a lexicon with emphasis on the odontocetes.
 Smithsonian Contributions to Zoology:1–249. DOI: 10.5479/si.00810282.627.
- Mourlam MJ, Orliac MJ. 2017. Infrasonic and Ultrasonic Hearing Evolved after the Emergence of Modern Whales. *Current Biology* 27:1776-1781.e9. DOI: 10.1016/j.cub.2017.04.061.
- Muizon C de. 1988a. Les relations phylogénétiques des Delphinida (Cetacea, Mammalia).
 Annales de Paléontologie 74:159–227.
- Muizon C de. 1988b. Les vertébrés fossiles de la Formation Pisco (Pérou). Troisième partie: Les
 Odontocètes (Cetacea, Mammalia) du Miocène. *Travaux de l'Institut Français d'Etudes* Andines 78:1–244.
- Murakami M, Shimada C, Hikida Y, Hirano H. 2012. Two new extinct basal phocoenids
 (Cetacea, Odontoceti, Delphinoidea), from the upper Miocene Koetoi Formation of Japan
 and their phylogenetic significance. *Journal of Vertebrate Paleontology* 32:1172–1185.
 DOI: 10.1080/02724634.2012.694337.
- Murakami M, Shimada C, Hikida Y, Hirano H. 2014. Asymmetrical Basal Delphinoid Skull
 from the Upper Lower Miocene Yamato Formation of Hokkaido, Northern Japan:
 Implications on Evolution of Cranial Asymmetry and Symmetry in Odontoceti.
 Paleontological Research 18:134–149. DOI: 10.2517/2014pr013.
- Oishi M, Hasegawa Y, Yanagisawa Y, Matsubara T, Kikuchi H, Komori K, Kawamorita H.

 1999. Miocene kentriodontid dolphins from Ninohe and Ichinohe, Iwate Prefecture, Japan.



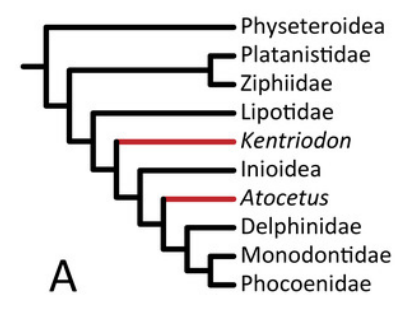
- 811 Abstract of the 1999 Annual Meeting of the Palaeontological Society of Japan:55. (January
- 812 29 31, 1999 at Sendai, Japan, Palaeontological Society of Japan). [Japanese]
- 813 Oishi M, Kawakami T. 1984. A new occurrence of desmostylian molar from the Miocene
- Kadonosawa Formation, Nisatai, Ninohe-City, Iwate Prefecture. *The Journal of the*
- 600 *Geological Society of Japan* 90(1):55–58. [Japanese]
- Peredo CM, Uhen MD, Nelson MD. 2018. A new kentriodontid (Cetacea: Odontoceti) from the
- early Miocene Astoria Formation and a revision of the stem delphinidan family
- Kentriodontidae. *Journal of Vertebrate Paleontology* 38. DOI:
- 819 10.1080/02724634.2017.1411357.
- Rensberger JM. 1969. A new iniid cetacean from the Miocene of California. *University of California publications in geological sciences* 82:43.
- 822 Salinas-Márquez FM, Barnes LG, Flores-Trujillo JG, Aranda-Manteca FJ. 2014. A species of
- fossil dolphin (Cetacea; Delphinoidea; Kentriodontoidae) from the Middle Miocene of Baja
- 824 California. *Boletin de la Sociedad Geologica Mexicana* 66:145–164. DOI:
- 825 10.18268/BSGM2014v66n1a11.
- 826 Tanaka Y, Abella J, Aguirre-Fernández G, Gregori M, Fordyce RE. 2017. A new tropical
- Oligocene dolphin from Montañita/Olón, Santa Elena, Ecuador. *PLoS ONE* 12:e0188380.
- B28 DOI: 10.1371/journal.pone.0188380.
- 829 Tanaka Y, Fordyce RE. 2014. Fossil dolphin Otekaikea marplesi (Latest Oligocene, New
- Zealand) expands the morphological and taxonomic diversity of oligocene cetaceans. *PLoS*
- 831 *ONE* 9. DOI: 10.1371/journal.pone.0107972.
- 832 Tanaka Y, Fordyce RE. 2016. Papahu-like fossil dolphin from Kaikoura, New Zealand, helps to
- fill the Early Miocene gap in the history of Odontoceti. New Zealand Journal of Geology
- *and Geophysics* 59:551–567. DOI: 10.1080/00288306.2016.1211540.
- 835 True FW. 1912. Description of a new fossil porpoise of the genus *Delphinodon* from the
- Miocene Formation of Maryland. Journal of the Academy of Natural Sciences of
- 837 *Philadelphia* 2:165–197.
- Tuzino T, Kudo T, Nakae S, Kondo R, Nishioka Y, Ueki T. 2018. Geology of the Ichinohe
- district. Quadrangle Series, 1:50,000, Geological Survey of Japan, AIST, 161p. [Japanese
- with English abstract]
- 841 TuZino T, Yanagisawa Y. 2017. Diatom occurence from the Miocene in the Ichinohe district,
- nothern part of Iwate Prefecture, NE Japan. *Bulletin of the Geological Survey of Japan*
- 68:237–258. [Japanese with English abstract]
- Whitmore FC, Kaltenbach JA. 2008. Neogene Cetacea of the Lee Creek Phosphate Mine, North
- Carolina. *Virginia Museum of Natural History Special Publication* 14:181–269.
- Yanagisawa Y, Akiba F. 1998. Refined Neogene diatom biostratigraphy for the northwest
- Pacific around Japan, with an introduction of code numbers for selected diatom biohorizons.
- The Journal of the Geological Society of Japan 104:395–414. DOI:
- 849 10.5575/geosoc.104.395.



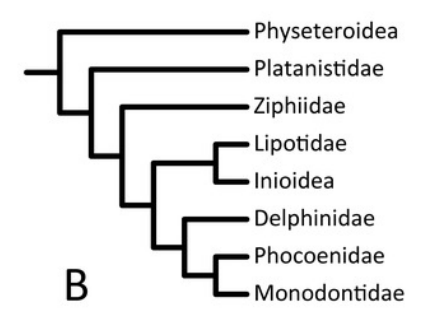
Several hypotheses of the phylogeny of the Delphinida.

Topologies have been modified from previous studies, all trees are unweighted and unordered. The kentriodontids lineages are colored red. (A) morphology tree from Geisler et al., 2011; Geisler, Godfrey & Lambert, 2012. (B) molecules tree from McGowen, Spaulding & Gatesy, 2009; McGowen et al., 2011; McGowen et al., 2020. (C) morphology tree from Murakami et al., 2012; Murakami et al., 2014. (D) morphology tree from Lambert et al., 2017; Peredo, Uhen & Nelson, 2018; Kimura & Hasegawa, 2019, using unconstrained search with combined morphology and molecular data. (E) morphology tree from Tanaka & Fordyce, 2014; Tanaka & Fordyce, 2016; Tanaka et al., 2017, using a molecules tree constrained. (F) morphology tree from this paper, using a molecules tree constrained.

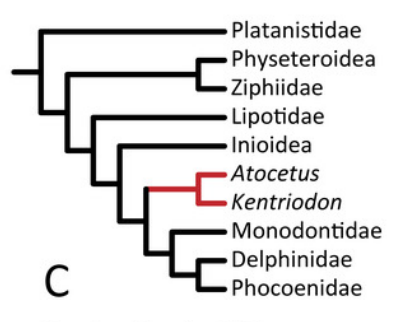




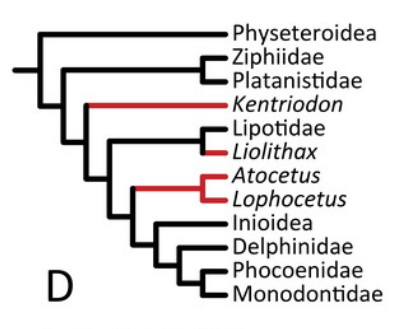
Geisler et al., 2011 Geisler, Godfrey & Lambert, 2012



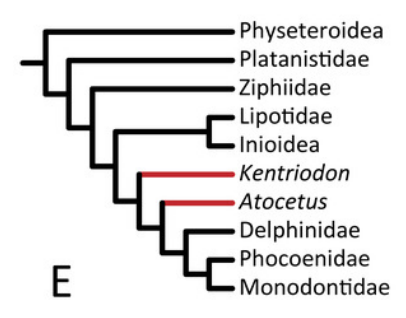
McGowen, Spaulding & Gatesy, 2009 McGowen et al., 2011 McGowen et al., 2020



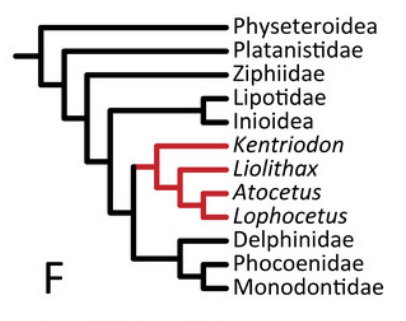
Murakami et al., 2012 Murakami et al., 2014



Lambert et al., 2017 Peredo, Uhen & Nelson, 2018 Kimura & Hasegawa, 2019



Tanaka & Fordyce, 2014 Tanaka & Fordyce, 2016 Tanaka et al., 2017



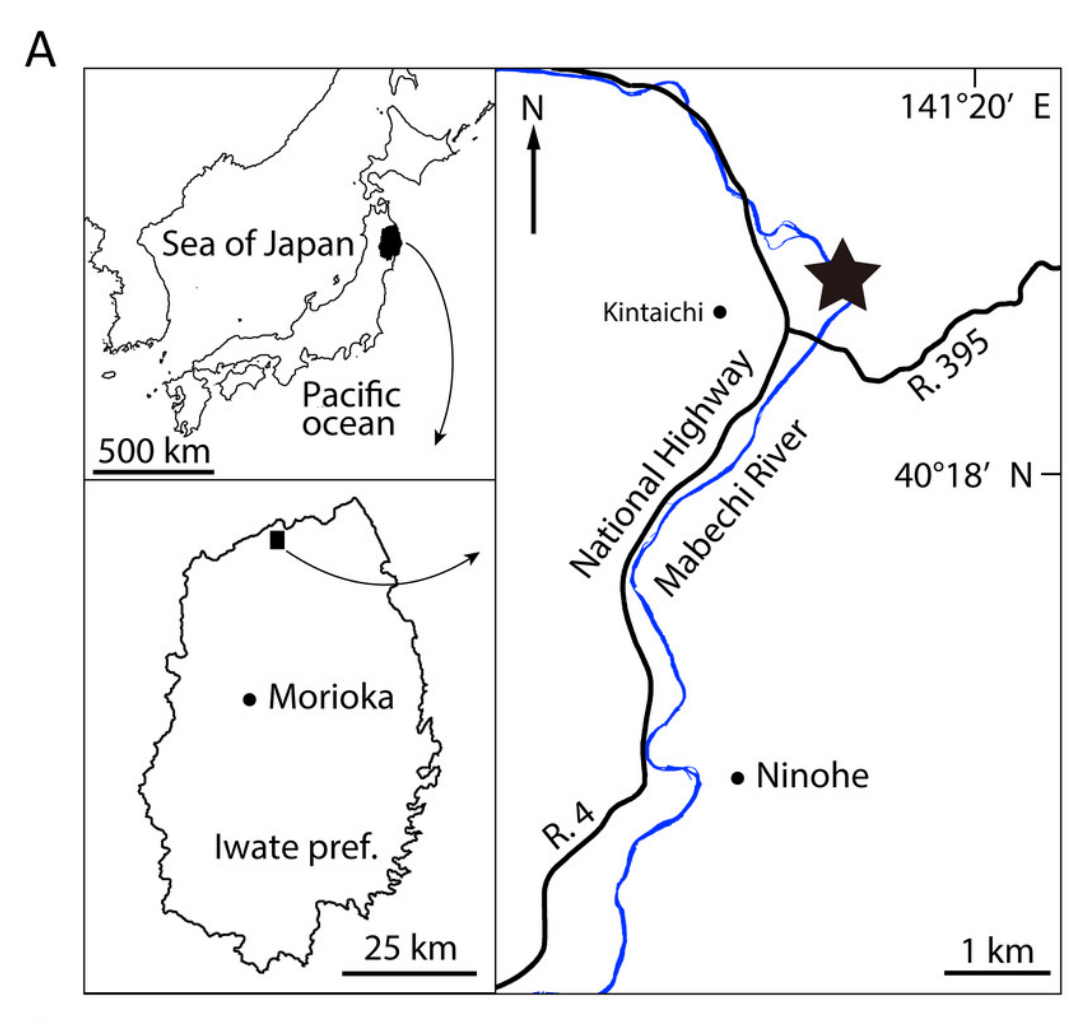
Guo & Kohno (this paper)

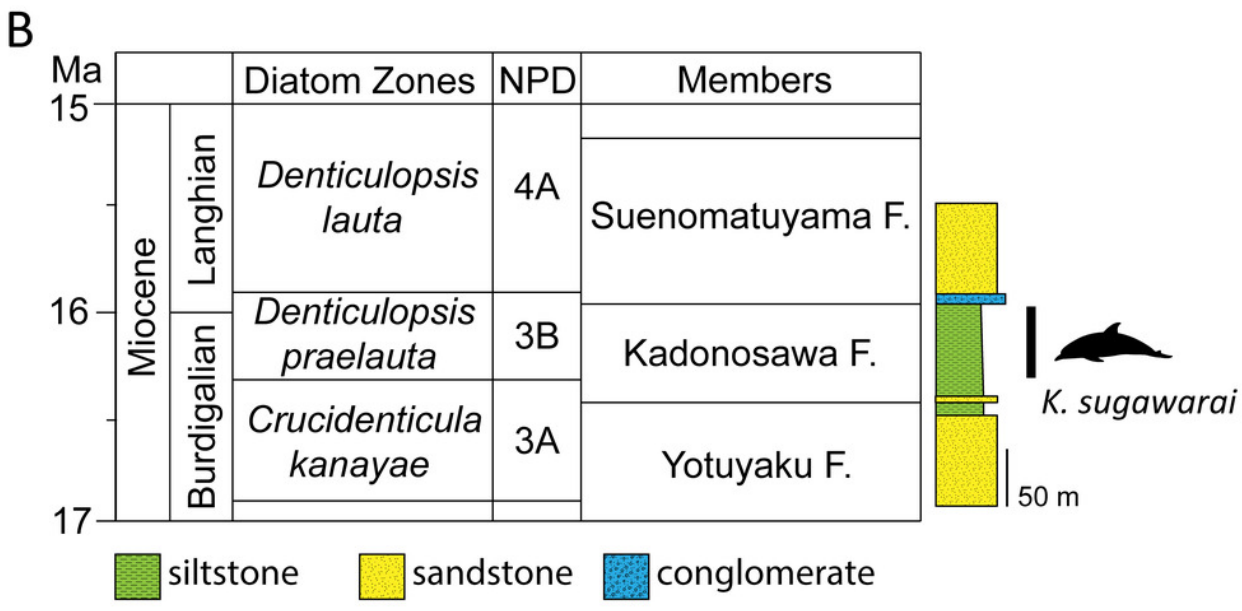


Geographic and geologic context of Kentriodon sugawarai locality.

(A) the type locality of *Kentriodon sugawarai*, sp. nov., holotype, NMHF 999. (B) left, diatom zone and stratigraphic diagram, modified from Tuzino & Yanagisawa (2017). right, stratigraphic column of the Mabechi River, Ninohe City, Iwate Prefecture, Japan.



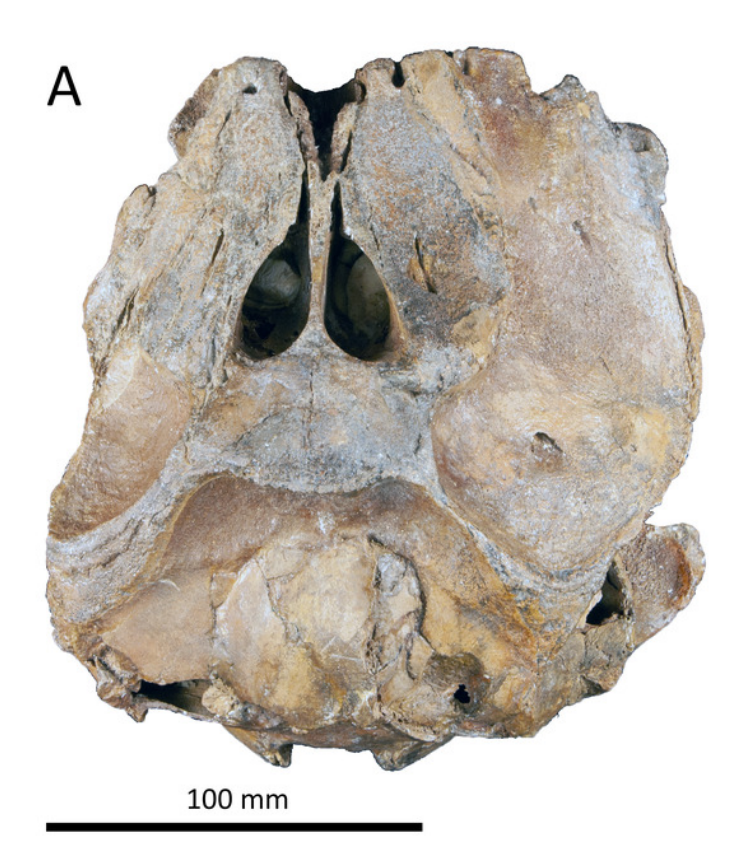


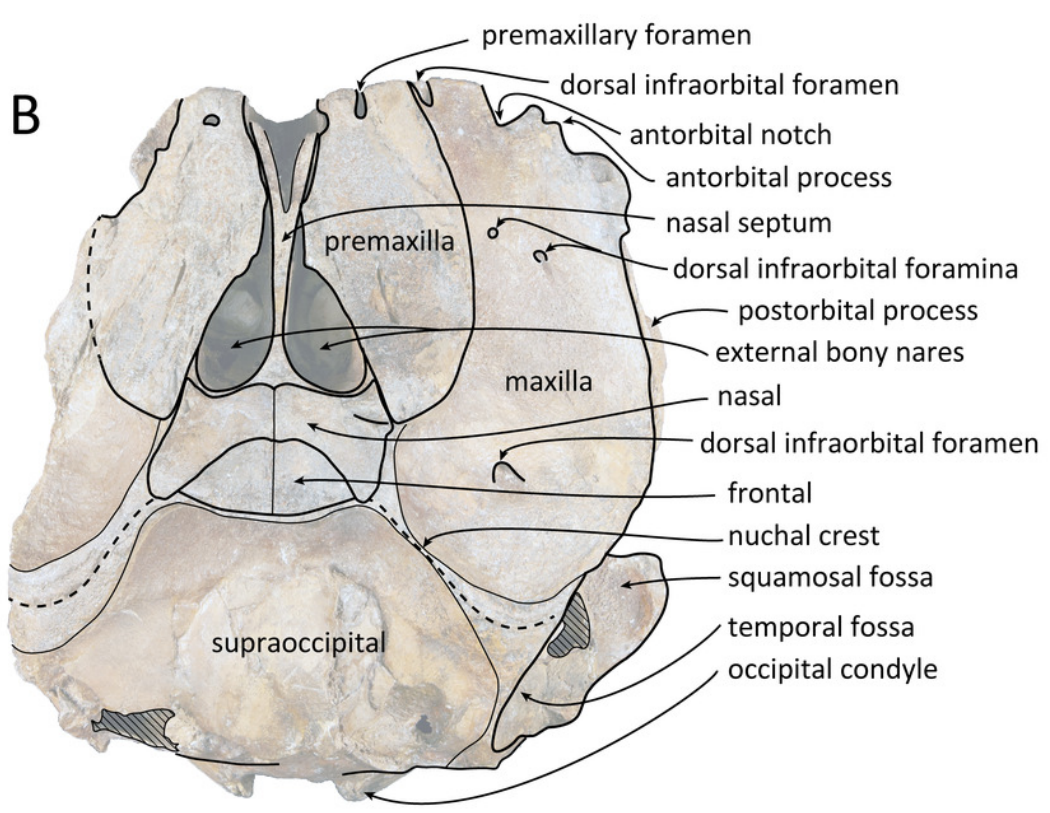




Dorsal views of the skull of Kentriodon sugawarai, sp. nov., holotype, NMHF 999.

(A) photo. (B) corresponding line drawing with anatomical interpretations. Scale bar equals 100 mm.

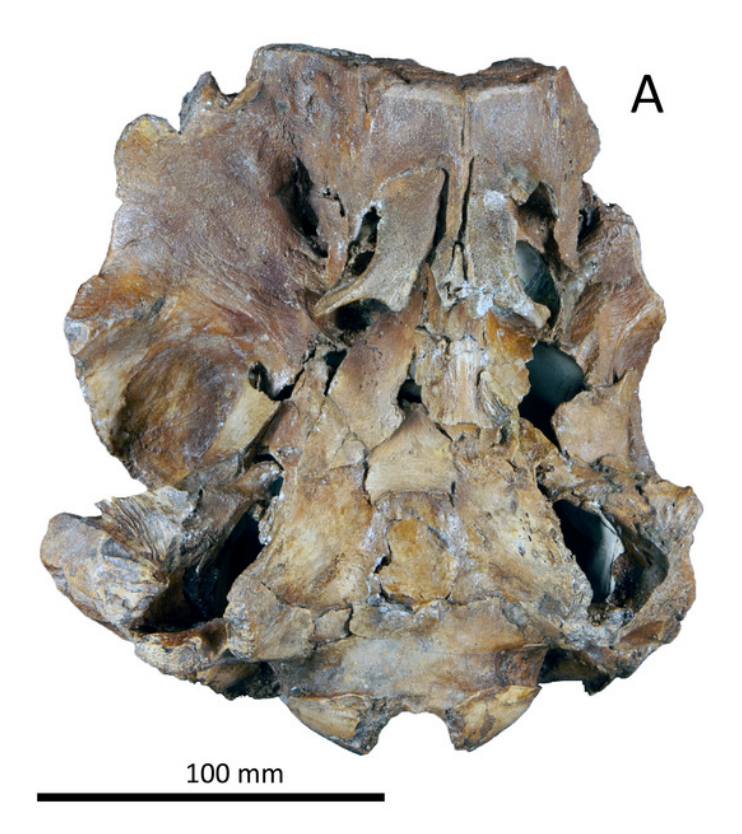


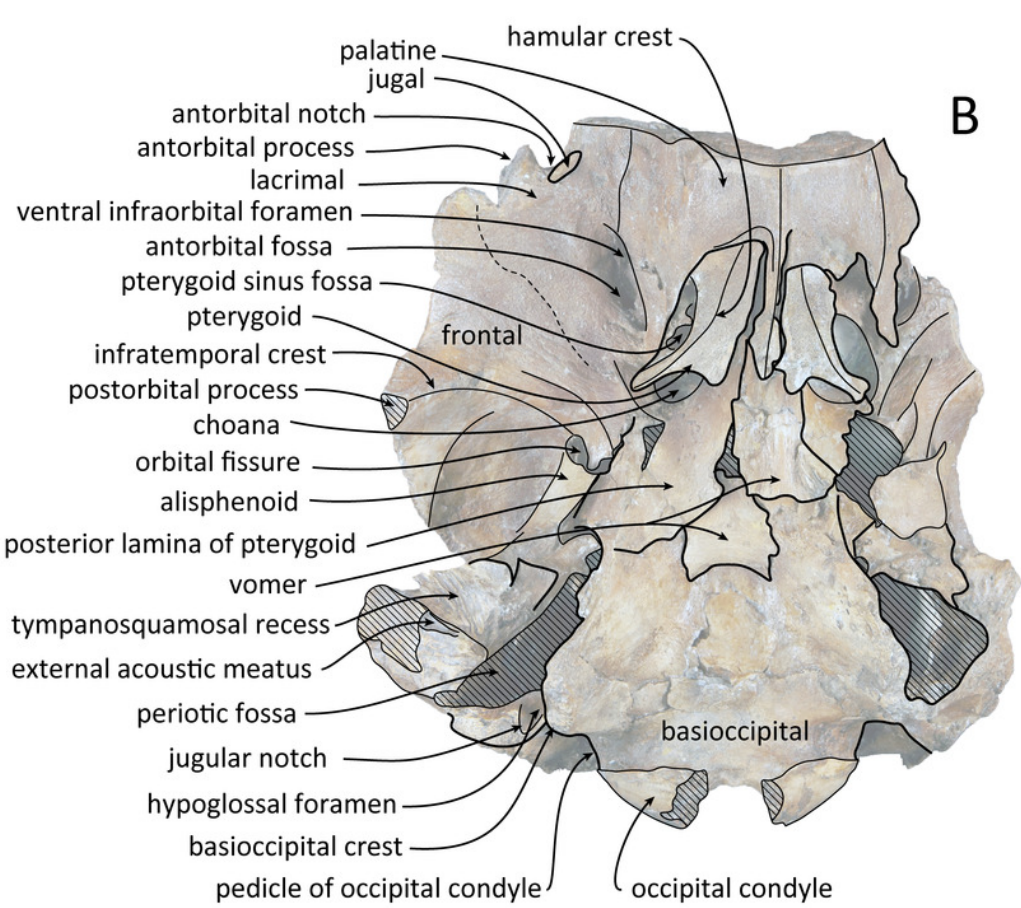




Ventral views of the skull of Kentriodon sugawarai, sp. nov., holotype, NMHF 999.

(A) photo. (B) corresponding line drawing with anatomical interpretations. Scale bar equals 100 mm.

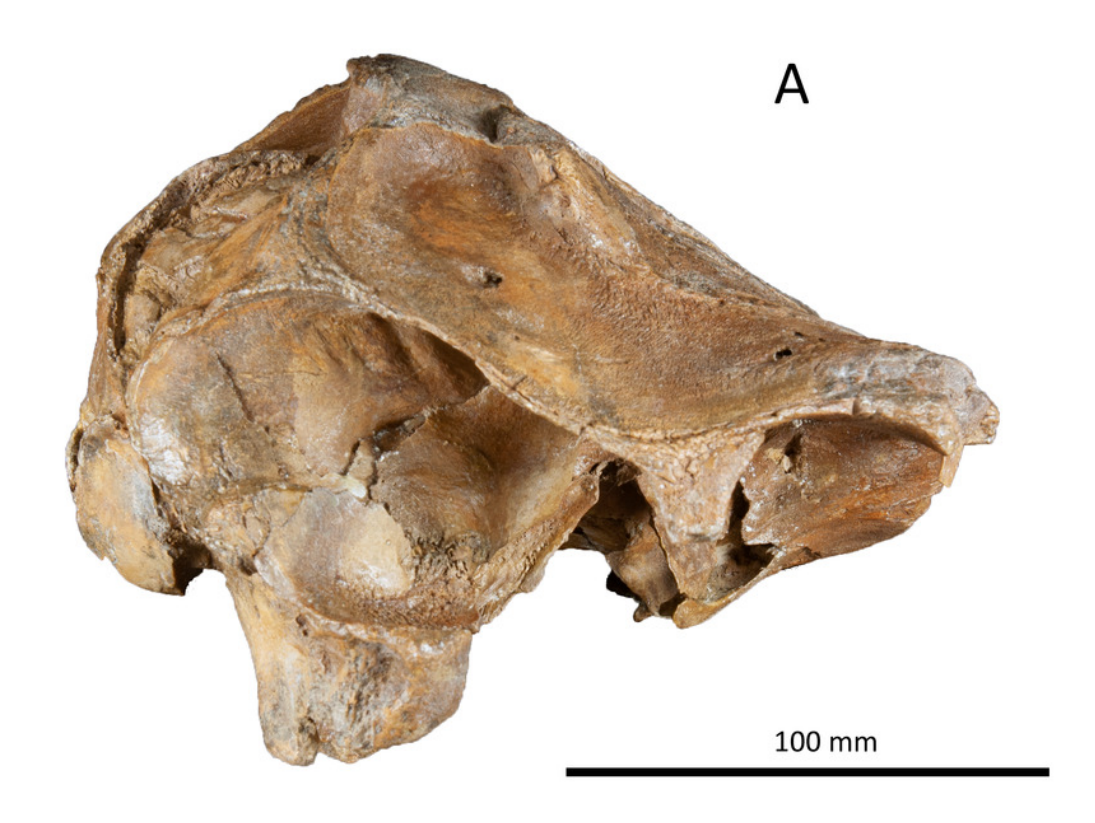


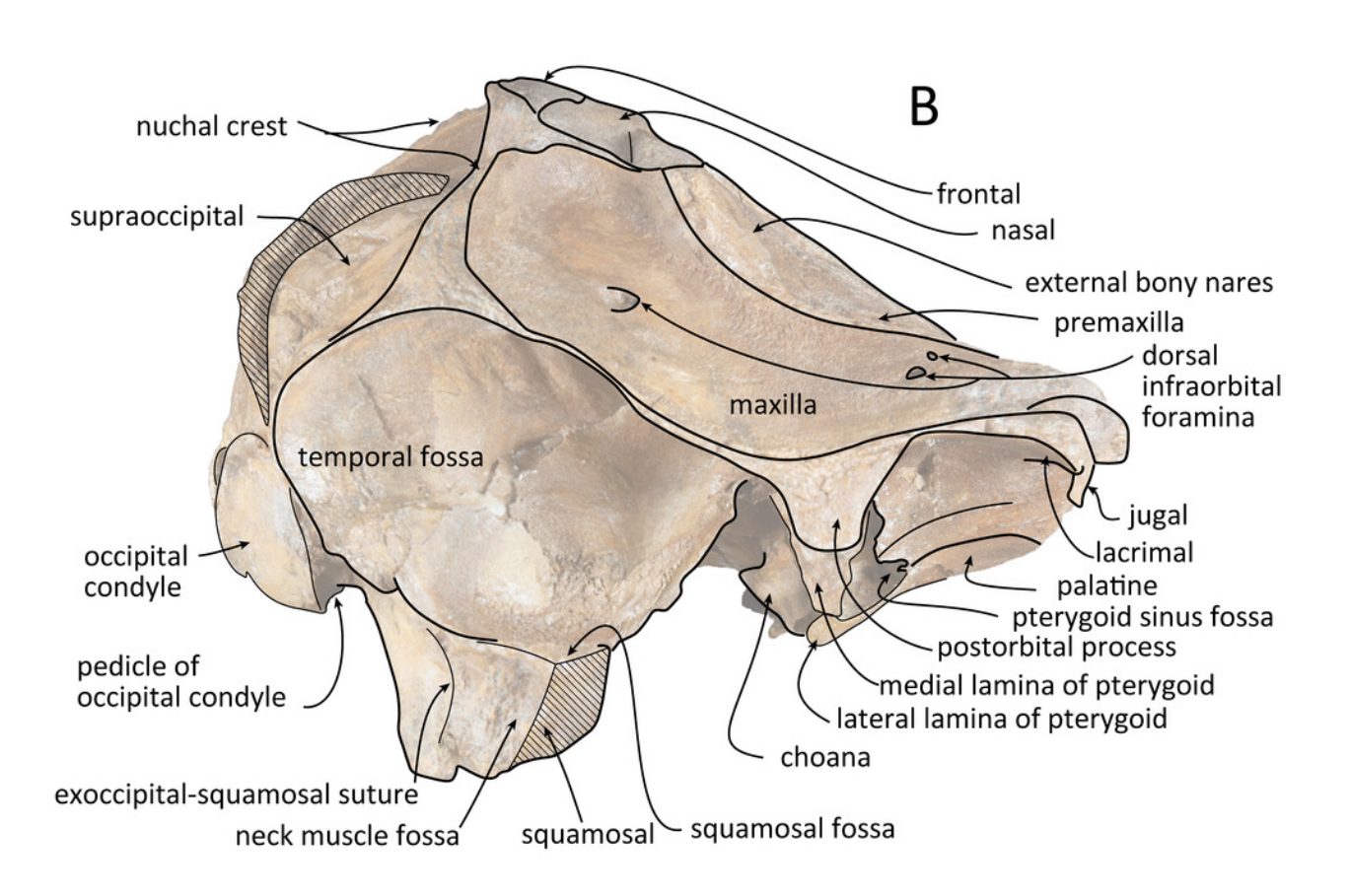




Right lateral views of the skull of Kentriodon sugawarai, sp. nov., holotype, NMHF 999.

(A) photo. (B) corresponding line drawing with anatomical interpretations. Scale bar equals 100 mm.

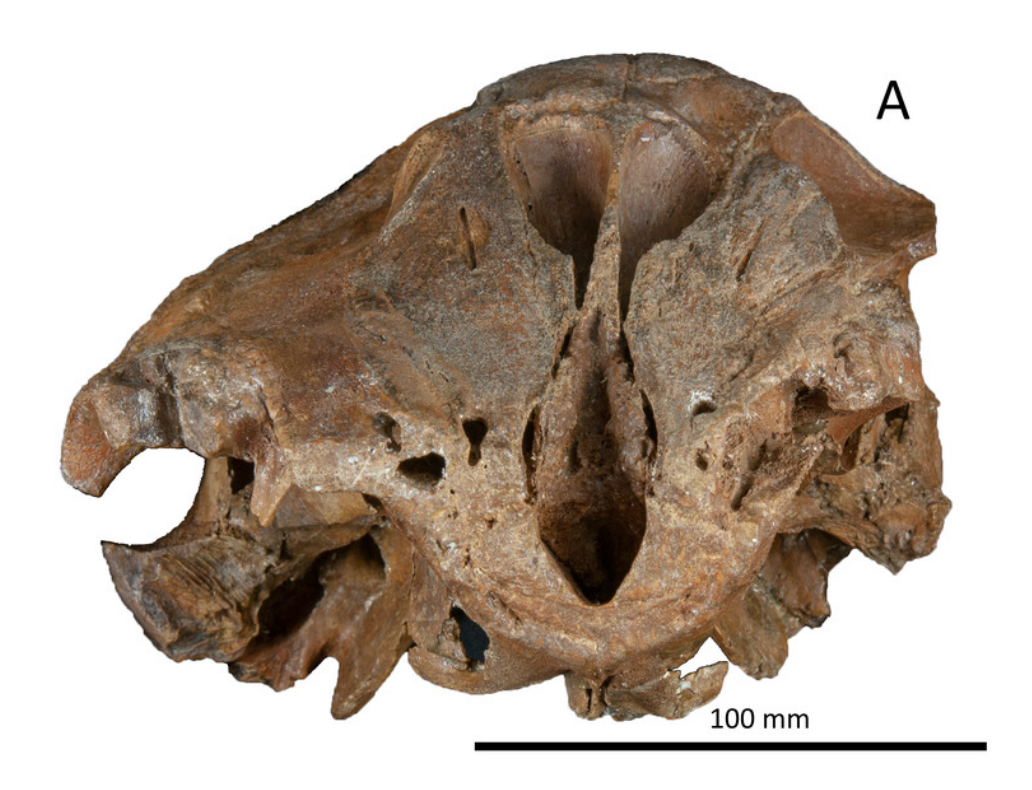


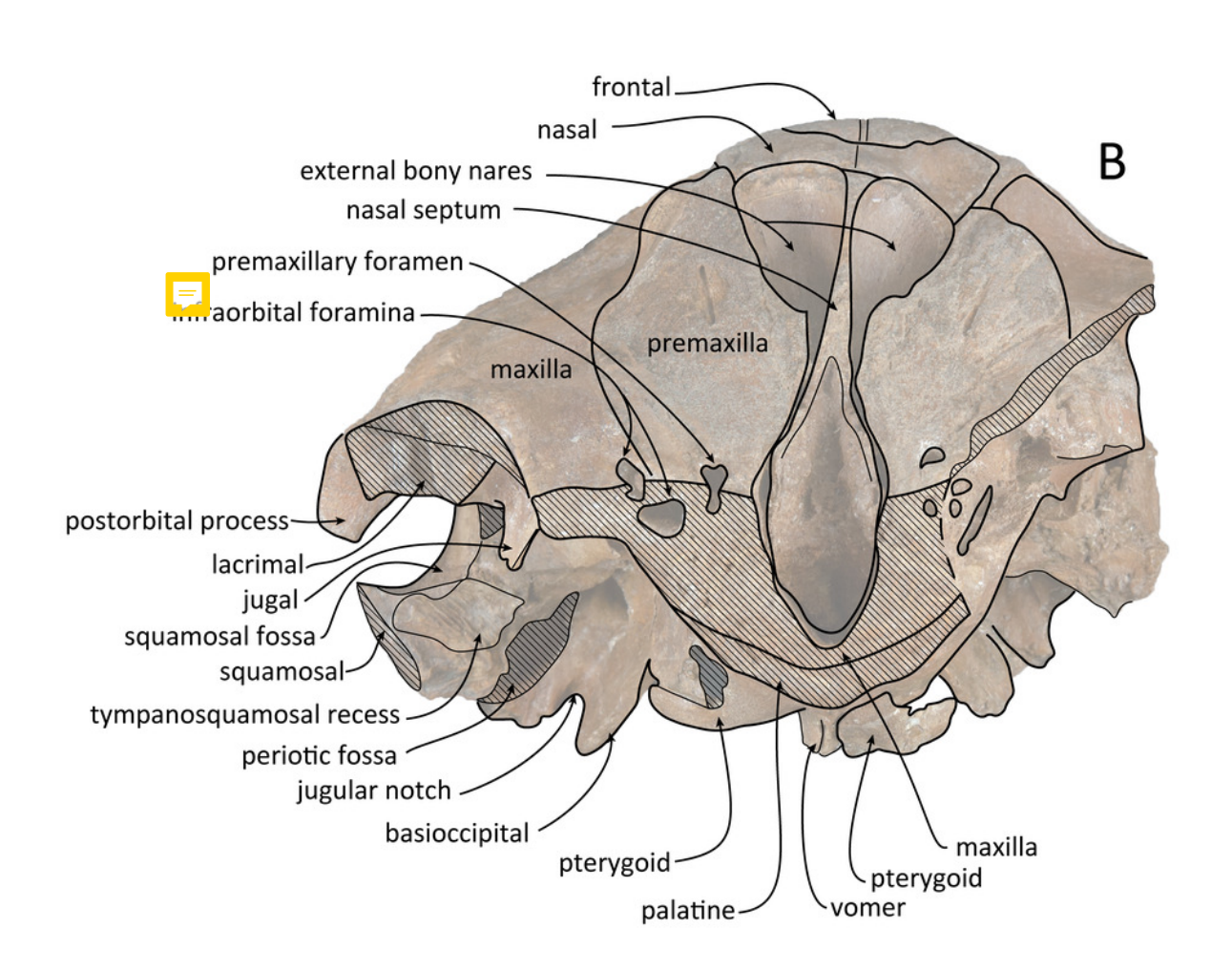




Anterior views of the skull of Kentriodon sugawarai, sp. nov., holotype, NMHF 999.

(A) photo. (B) corresponding line drawing with anatomical interpretations. Scale bar equals 100 mm.



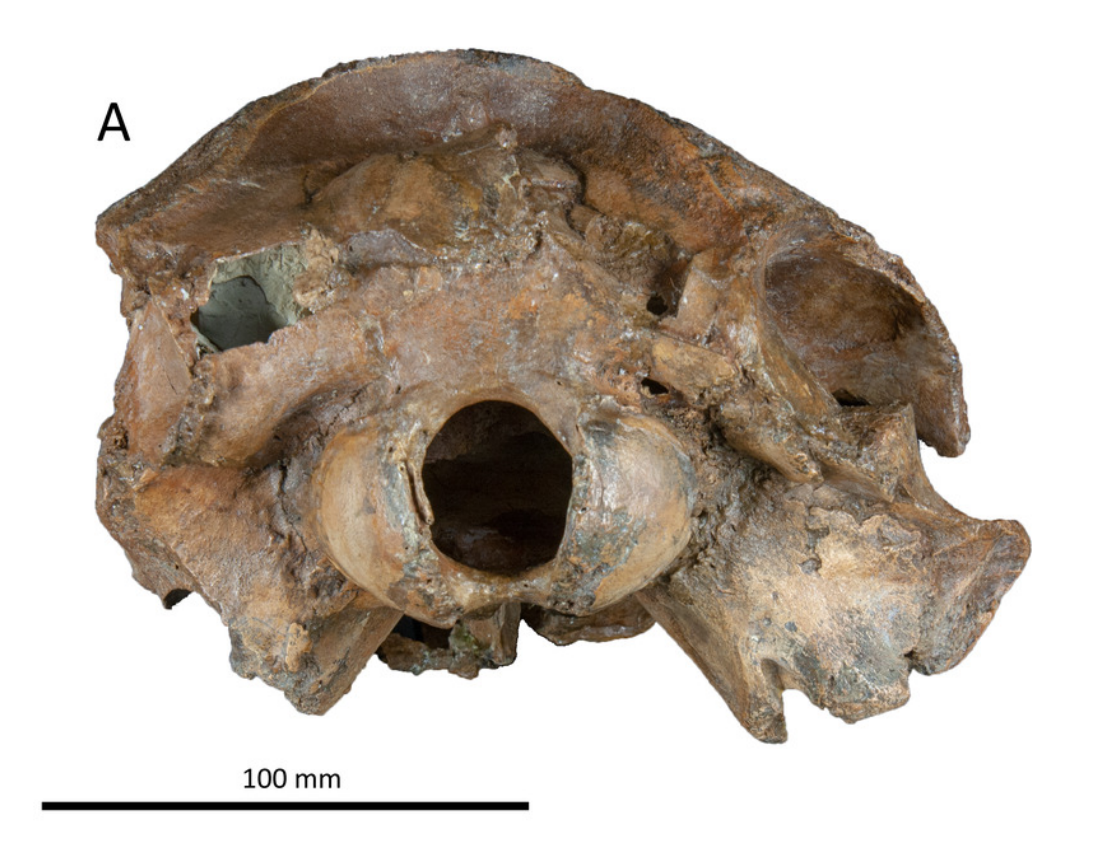


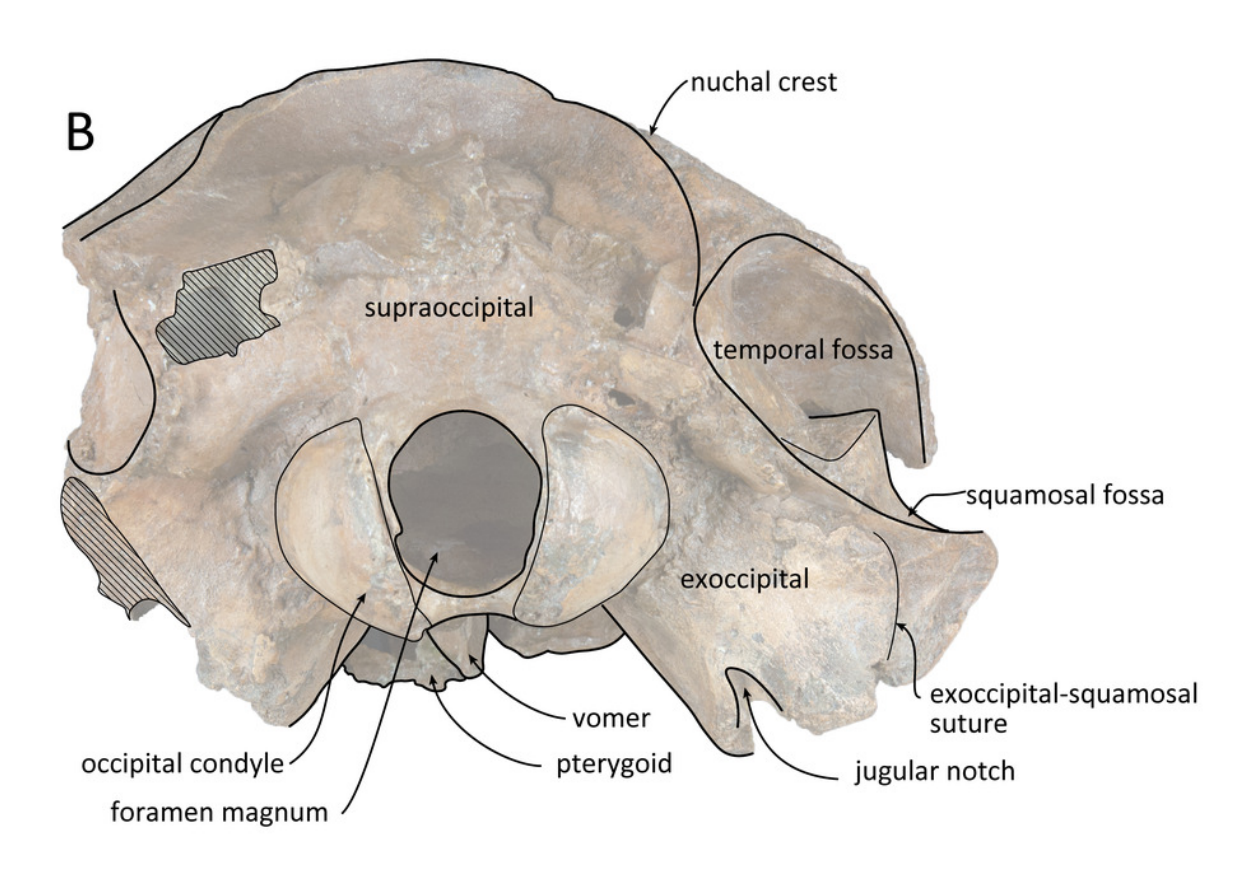


Posterior views of the skull of Kentriodon sugawarai, sp. nov., holotype, NMHF 999.

(A) photo. (B) corresponding line drawing with anatomical interpretations. Scale bar equals 100 mm.



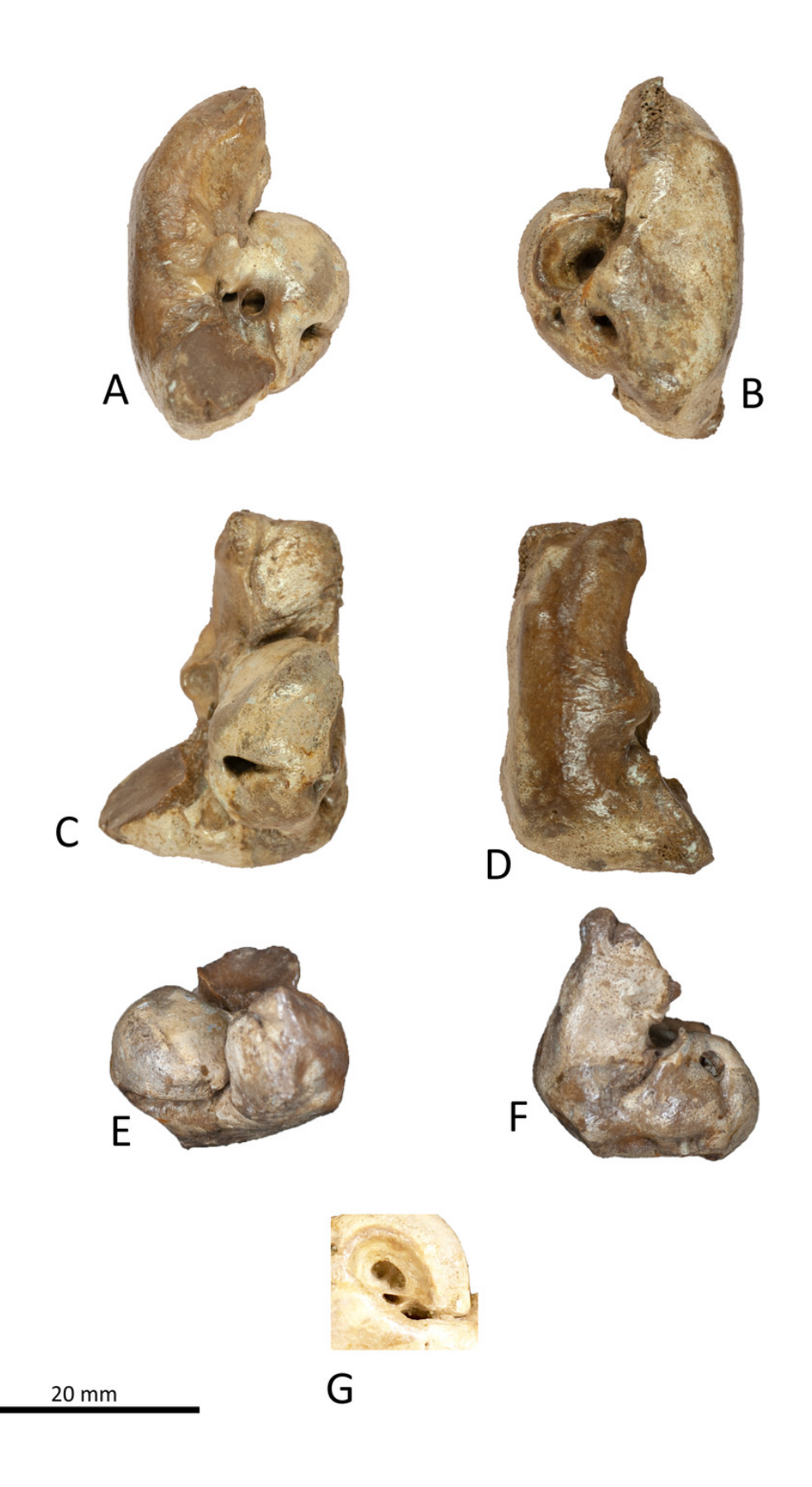






Right periotic of Kentriodon sugawarai, sp. nov., holotype, NMHF 999.

(A) ventral view. (B) dorsal view. (C) medial view. (D) lateral view. (E) anterior view. (F) posterior view. (G) a specific view at the internal acoustic meatus. Scale bar equals 20 mm.

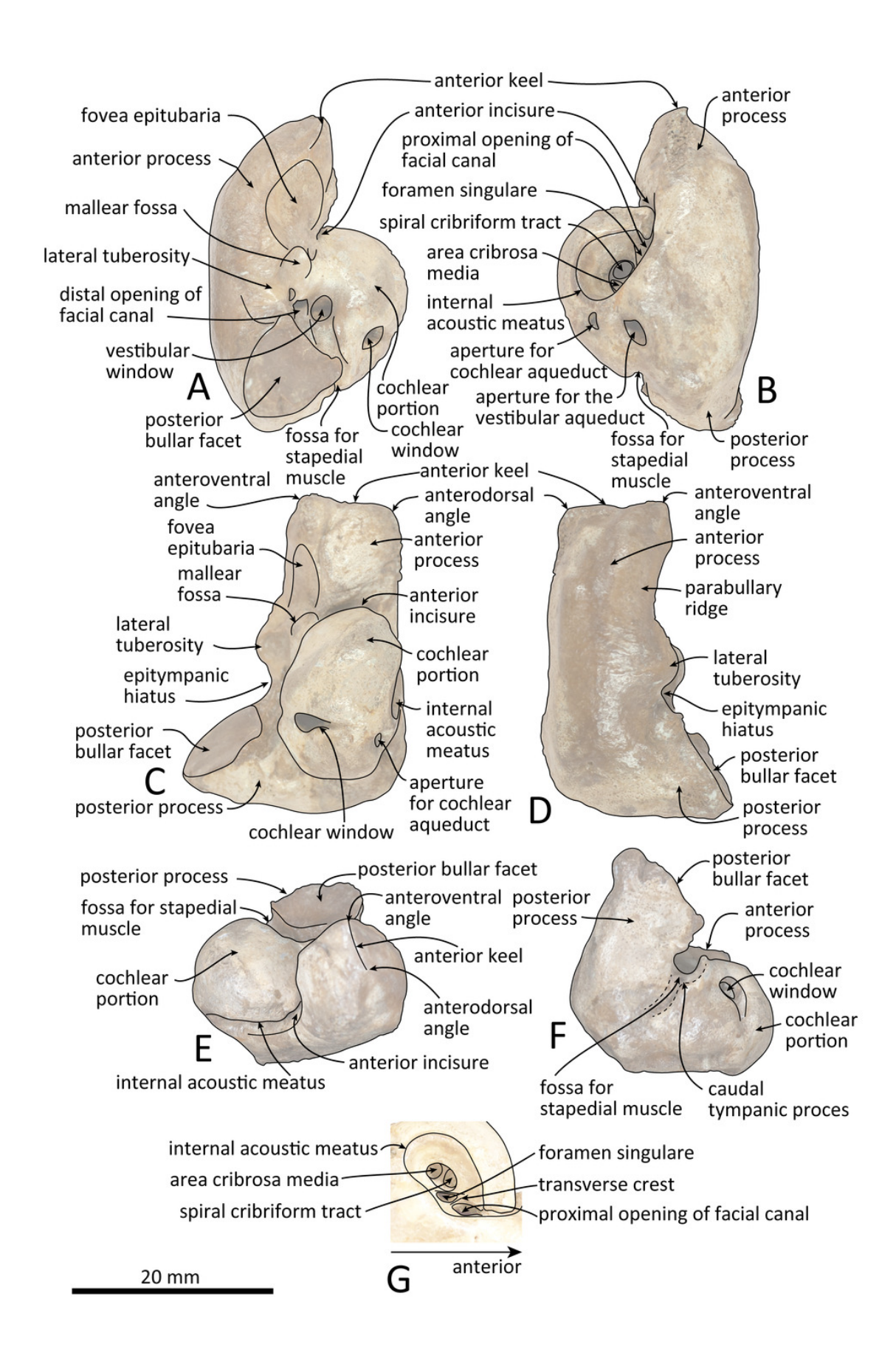




Line drawings of the right periotic of *Kentriodon sugawarai*, sp. nov., holotype, NMHF 999, with anatomical interpretations.

(A) ventral view. (B) dorsal view. (C) medial view. (D) lateral view. (E) anterior view. (F) posterior view. (G) a specific view at the internal acoustic meatus. Scale bar equals 20 mm.

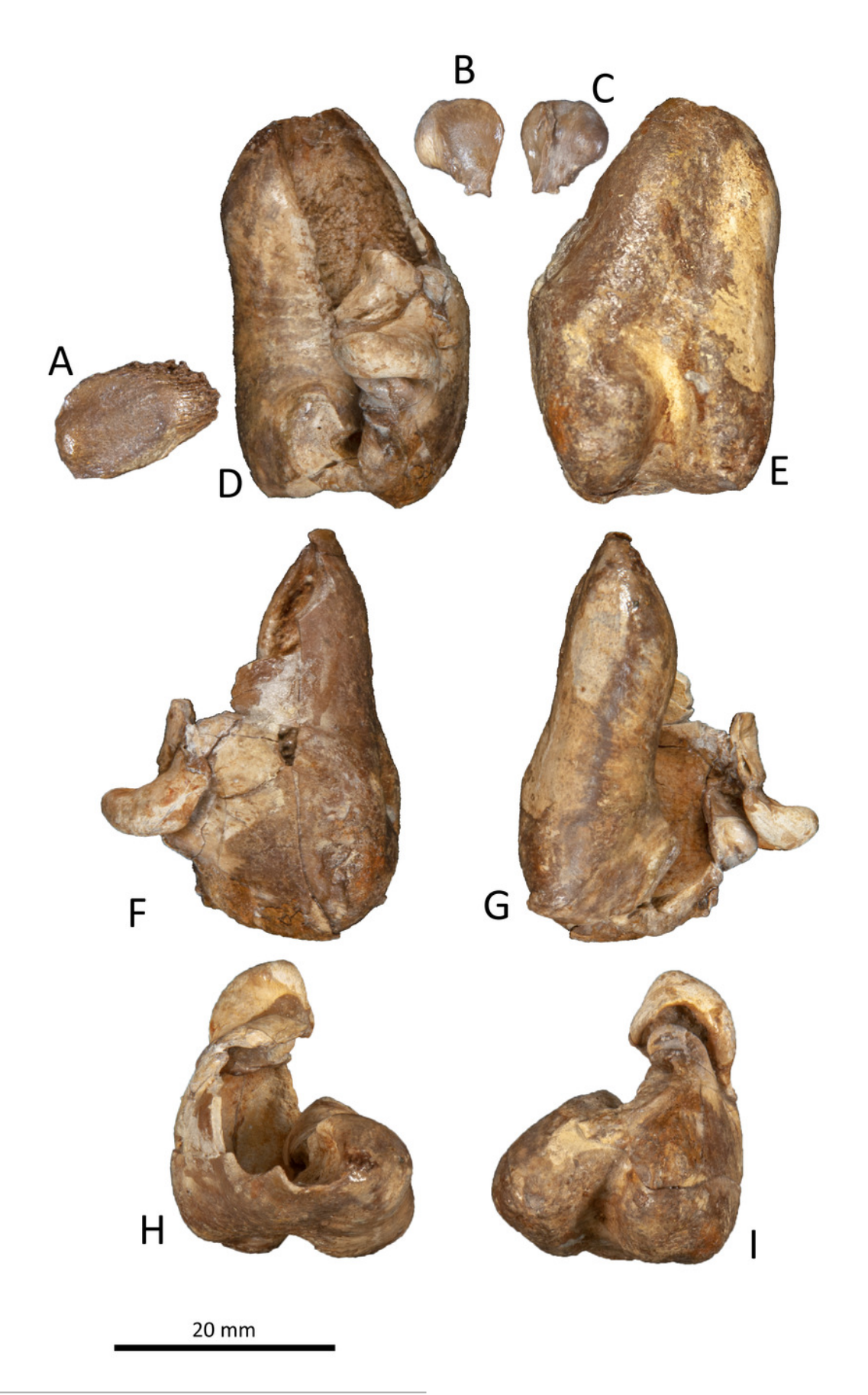






Right tympanic bulla of Kentriodon sugawarai, sp. nov., hototype, NMHF 999.

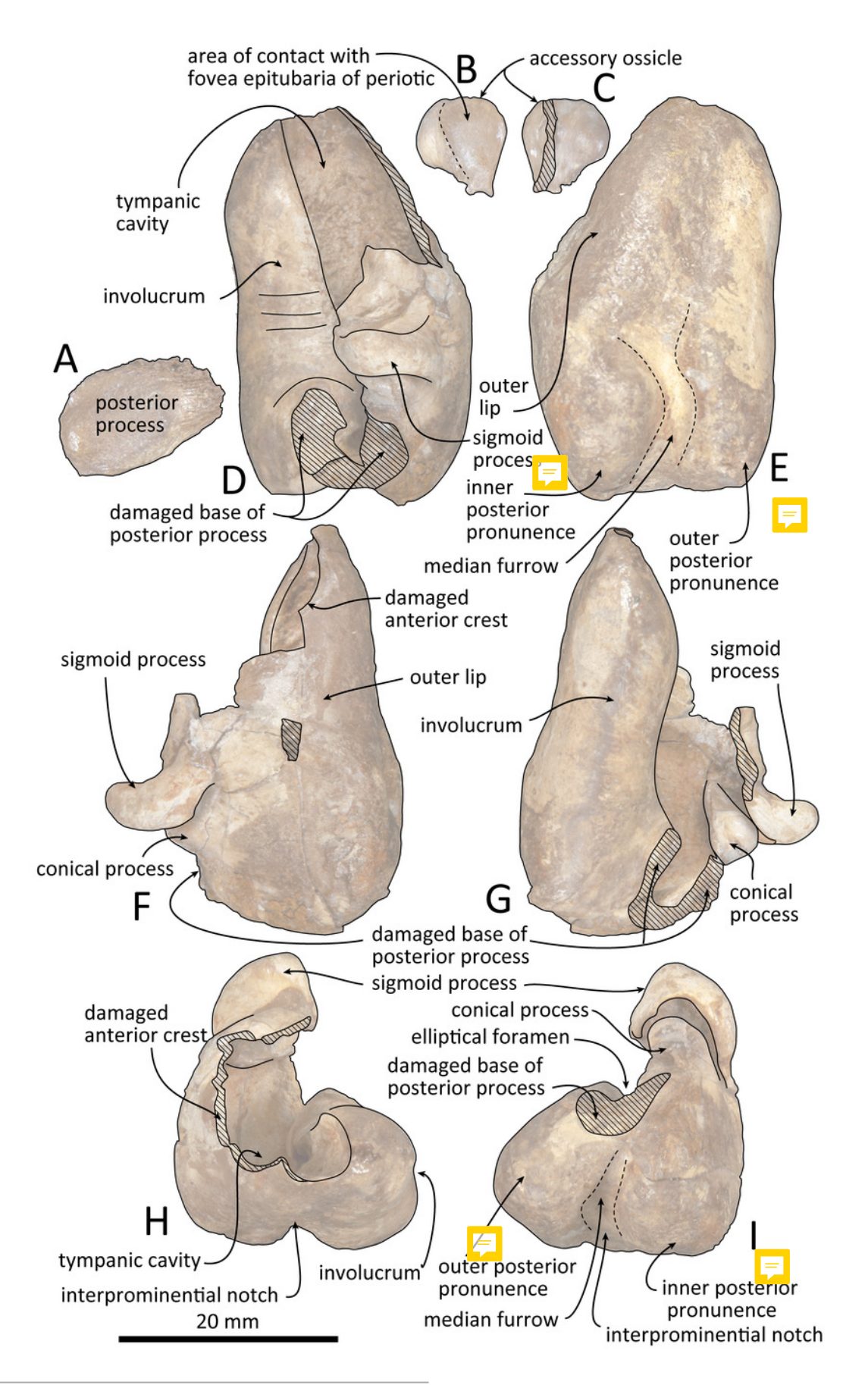
(A) dorsal view of the posterior process of the tympanic bulla. (B-C) accessory ossicle. (B) dorsal view. (C) ventral view. (D-I), left tympanic bulla. (D) dorsal view. (E) ventral view. (F) lateral view. (G) medial view. (H) anterior view. (I) posterior view. Scale bar equals 20 mm.





Line drawings of the right tympanic bulla of *Kentriodon sugawarai*, sp. nov., holotype, NMHF 999.

(A) dorsal view of the posterior process of the tympanic bulla. (B-C) accessory ossicle. (B) dorsal view. (C) ventral view. (D-I) left tympanic bulla. (D) dorsal view. (E) ventral view. (F) lateral view. (G) medial view. (H) anterior view. (I) posterior view. Scale bar equals 20 mm.

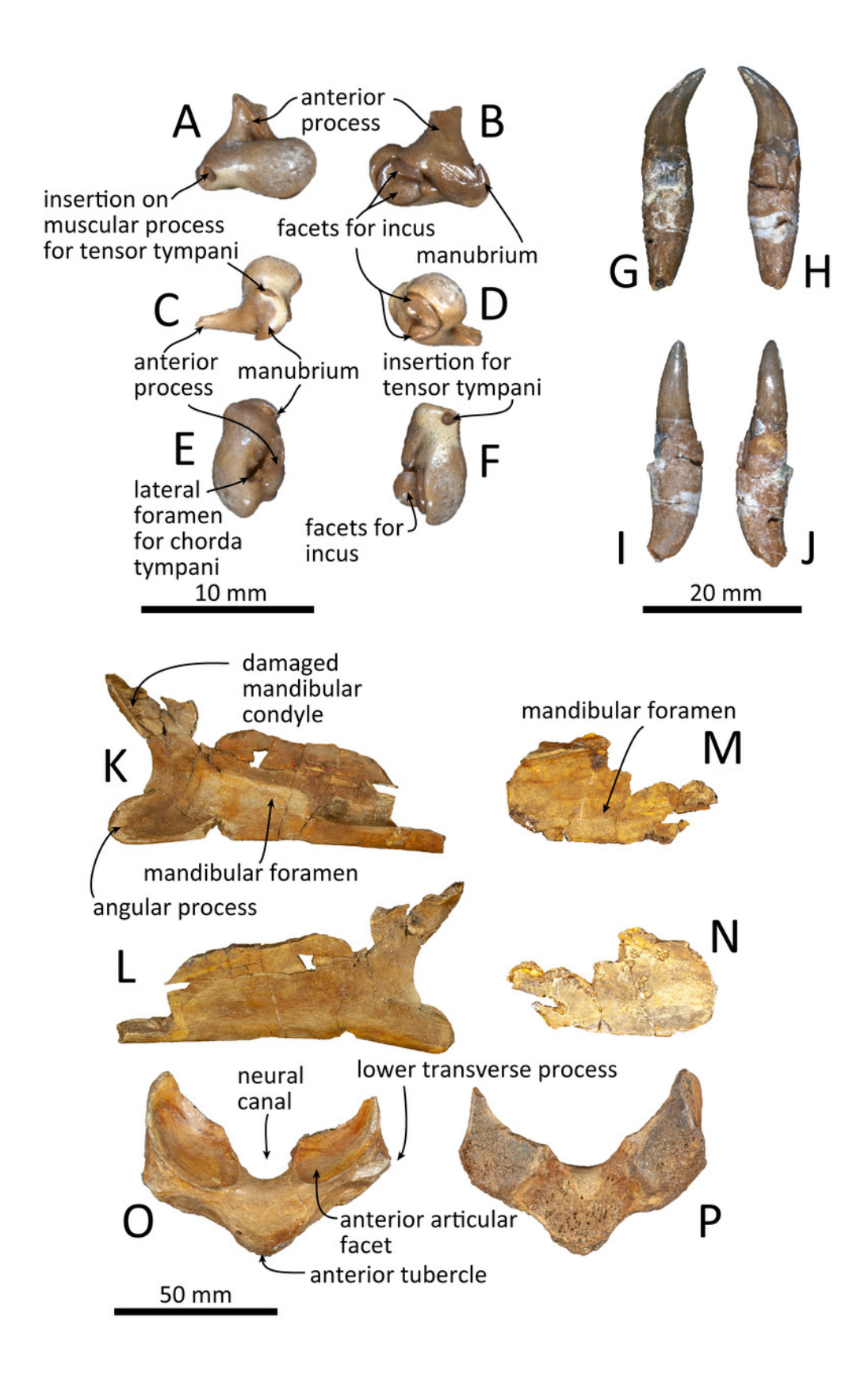




Malleus, tooth, mandible and vertebra of *Kentriodon sugawarai*, sp. nov., holotype, NMHF 999, with anatomical interpretations.

(A–F) right malleus. (A) ventral view. (B) dorsal view. (C) medial view. (D) lateral view. (E) anterior view. (F) posterior view. (G–J) probable upper tooth. (G) distal view. (H) mesial view. (I) lingual view. (J) labial view. (K–L) ascending ramus of the left mandible. (K) medial view. (L) lateral view. (M–N) horizontal ramus of the right mandible. (M) lingual view. (N) labial view. (O–P) ventral half of the atlas. (O) anterior view. (P) posterior view. Scale bar equals 20 mm.



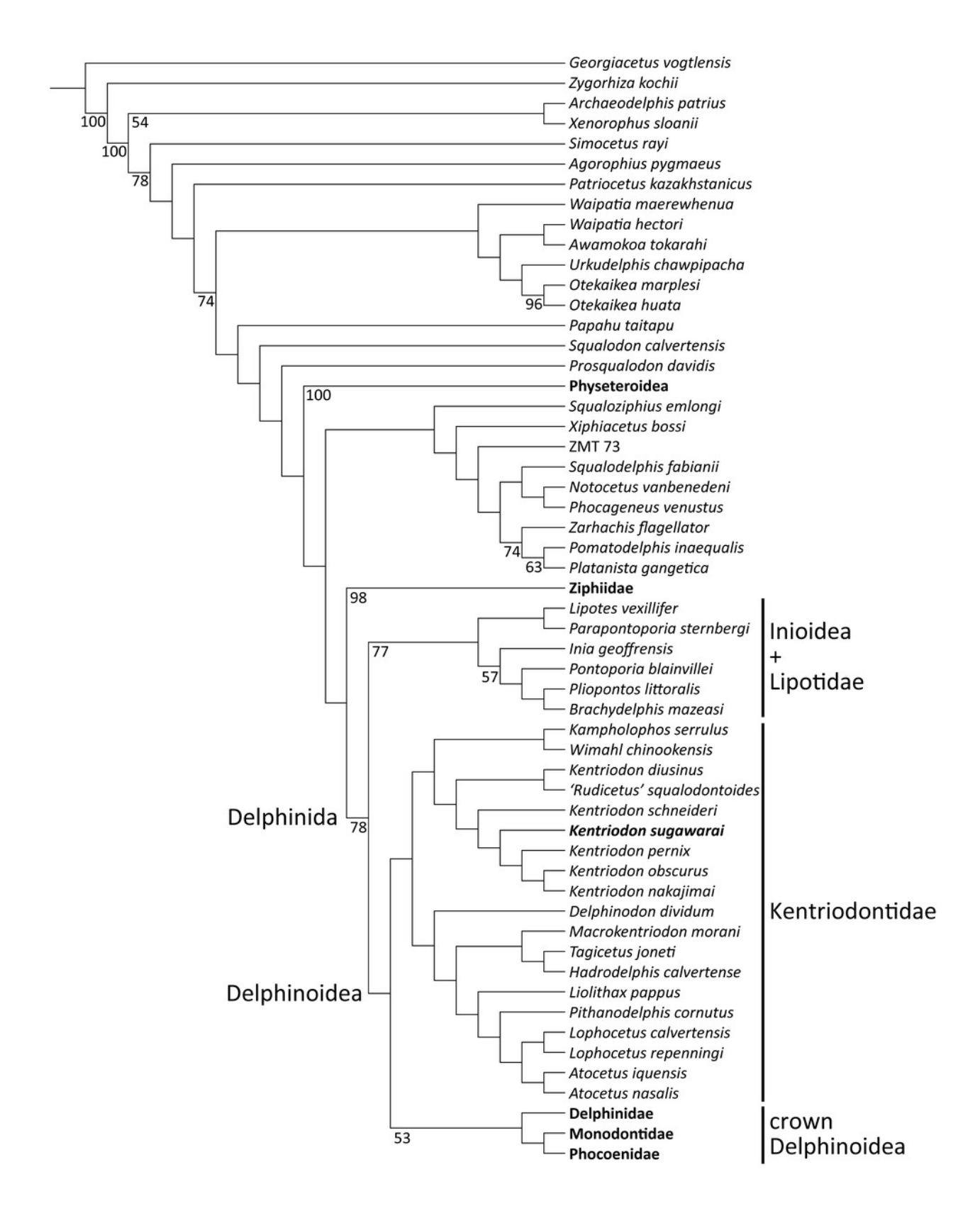




50% majority consensus tree showing the phylogenetic relationships of *Kentriodon sugawarai*, sp. nov.

50% majority consensus tree resulting from 256 most parsimonious trees with trees constraint by the molecular consensus tree from McGowen, Spaulding & Gatesy (2009), McGowen et al. (2011) and McGowen et al. (2020), 3424 steps long, with the consistency index = 0.197 and the retention index = 0.564. Numbers below nodes indicate bootstrap values (1,000 replicates). The values lower than 50% were omitted. The interspecific relationships within clades Physeteroidea, Ziphiidae, Delphinidae, Phocoenidae, and Monodontidae were omitted and these groups were collapsed to families/superfamilies...







Strict consensus tree showing the phylogenetic relationships of *Kentriodon sugawarai*, sp. nov.

Strict consensus tree resulting from 256 most parsimonious trees with trees constraint by the molecular consensus tree from McGowen, Spaulding & Gatesy (2009), McGowen et al. (2011) and McGowen et al. (2020), 3424 steps long, with the consistency index = 0.197 and the retention index = 0.564. The interspecific relationships within clades Physeteroidea, Ziphiidae, Delphinidae, Phocoenidae, and Monodontidae were omitted and these groups were collapsed to families/superfamilies.



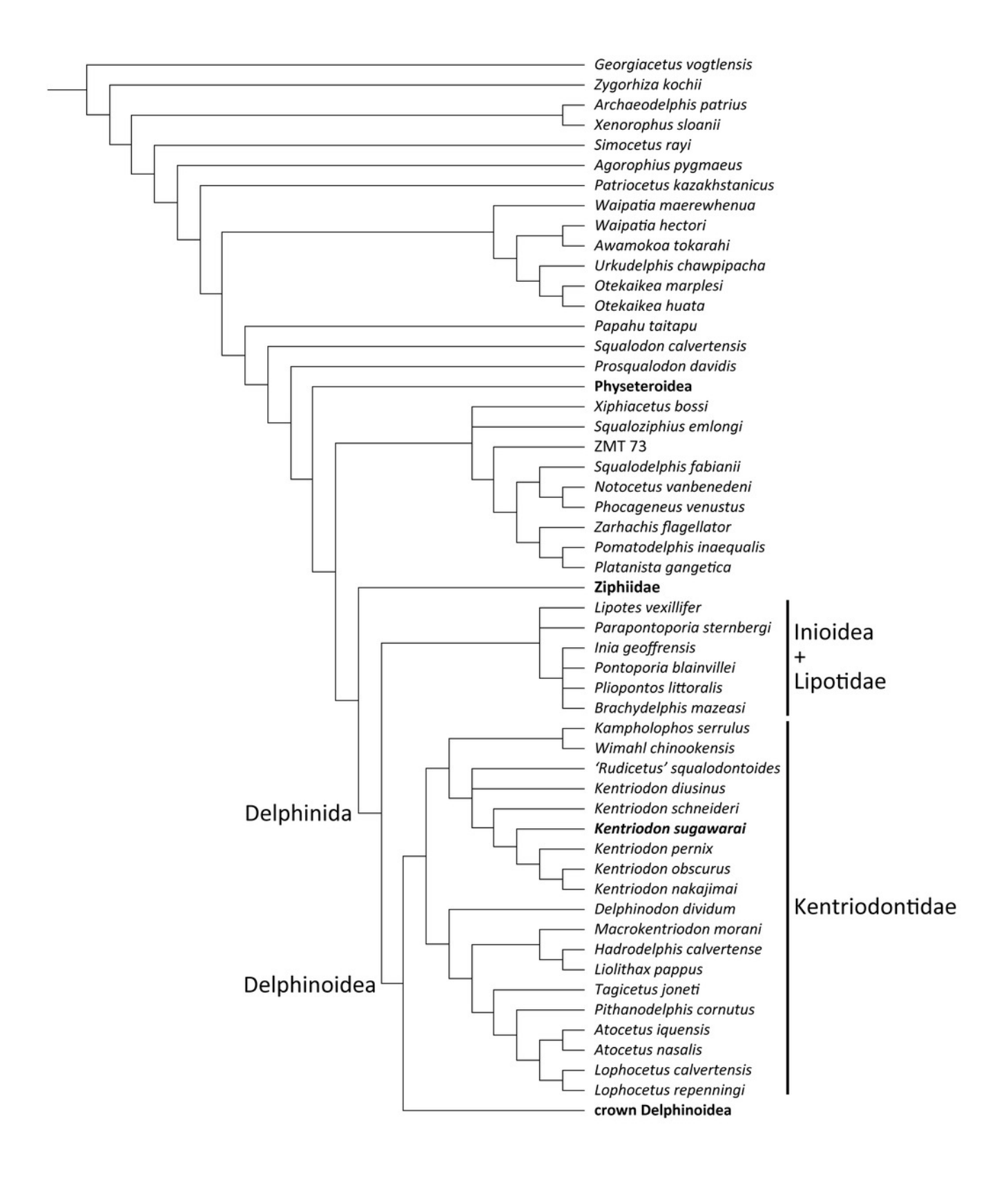




Table 1(on next page)

Measurements (in mm) for the skull and tympanoperiotic of *Kentriodon sugawarai* sp. nov., holotype, NMHF 999.

Abbreviations: e, estimate; +, not complete.



Dimension	Measurement
Skull	
Condylobasal length, from tip of rostrum to hindmost margin of occipital condyles	186.2+
Length of rostrum, from tip to line across hindmost limits of antorbital notches	15.1+
Width of rostrum at base, along line across hindmost limits of antorbital	107.2e
notches	
Maximum length of frontal at the vertex	19.3
Width of the foramen magnum	21.8
Width of premaxillae at posterior extremity	61.4
Width of nasal bones	53.4
Distance from tip of rostrum to external nares (to mesial end of anterior margin	56.0+
of right naris)	
Distance from tip of rostrum to internal nares (to mesial end of posterior	56.8+
margin of right pterygoid)	
Greatest preorbital width	181.2e
Greatest postorbital width	215.0e
Least supraorbital width	179.2e
Greatest width of external nares	41.8
Greatest width across zygomatic processes of squamosals	161.0+
Greatest width of premaxillae	101.4e
Greatest parietal width	138.0+
Greatest length of left temporal fossa, measured to external margin of temporal	110
crest	
Greatest width of left temporal fossa perpendicular to greatest length	54.5
Major diameter of left temporal fossa proper	41.6
Minor diameter of left temporal fossa proper	48.1+
Distance from foremost end of junction between nasals to hindmost point of	34.6
margin of nuchal crest	
Length of left orbit-from apex of preorbital process of frontal to apex of	52.4
postorbital process	1.0
Length of antorbital process of left lacrimal	18+
Greatest width of internal nares	71.4e
Greatest length of left pterygoid	47.6
Width across occipital condyles	70.5
Periotic	21.7
Total length	31.7
Length of anterior process	17.8
Width at pars cochlearis	13.2
Length of posterior bullar facet	10.5
Width of posterior bullar facet	9.9
Length of pars cochlearis, from anterior to posterior margin	17.2
Tympanic Bulla	27.4
Total length without posterior process as preserved	37.4
Total width as preserved	21.8
Width of inner posterior prominence	9.5



PeerJ

Atlas	
Width of atlas	69.1
Length of atlas	62.9+
Greatest width of facet for occipital condyle	24.9
1	